1
Designing Polymer Properties

Markus Gahleitner and John R. Severn

1.1
Polyolefins

Polyolefins represent approximately 50% by weight of all commodity and commodity-plus polymers, which in turn amount to about 90% by weight of the global polymer production. Literally hundreds of polyolefin grades are available commercially with an incredible variety of properties and applications, ranging from ultra-rigid thermosets (stiffer than steel, but with the premium of a much lower density) to high-performance elastomers via all conceivable thermoplastic and elastoplastic materials in between. Yet, if one looks at the chemical composition, polyolefins are surprisingly limited: polyethylene, polypropylene, a few copolymers of ethene with propene or another alpha-olefin, and little else. The key reason for this apparent contradiction is the unique and thorough molecular control of the polymerization process that modern transition metal-based catalysts are able to provide. With a proper choice of catalyst system and reaction conditions, it is possible to produce polyolefin materials with precisely defined and tunable chain microstructures and molecular mass distributions; this translates into a correspondingly fine control of the way in which such chains crystallize (when they are able to) and flow. In addition, a rich "toolbox" for supramolecular material design provides almost unlimited possibilities of further tailoring and diversification by means of intelligent processing, blending and additives formulations and technologies.

The result is an unprecedented success story, demonstrated by the exponential growth curve of polyolefin world consumption from less than 100 KT per annum during the mid-1950s to the current 100 Mt. It is worthy to add here that polyolefins should be considered as a metastable state of the light fractions of refined oil. Rather than flaring them, as has happened in the past, these are temporarily solidified, used for all forms of smart applications at a nominal cost, and burned afterwards to produce energy (the most logical way of recycling/disposing). If this was understood by politicians, environmentalists and opinion-makers, polyolefins would be recognized for what they are, namely the greenest and most environmentally friendly materials ever invented.

Tailor-Made Polymers. Via Immobilization of Alpha-Olefin Polymerization Catalysts.
Edited by John R. Severn and John C. Chadwick

ISBN: 978-3-527-31782-0

For almost three decades, the industrial production of high-density polyethylene (HDPE) and isotactic polypropylene (iPP) was based exclusively on heterogeneous catalysts (of the Ziegler–Natta or Phillips type) characterized by many different and ill-defined active species. Although massive research effort resulted in major improvements of catalytic performance, it is fair to admit that the approach was purely empirical.

It was only during the early 1980s that the serendipitous discovery of methylalumoxane as an effective activator of metallocene precatalysts made it possible to develop the first industrially appealing homogeneous ethene polymerization catalysts. Soon after that, with the implementation of stereorigid *ansa*-metallocenes with chirotopic sites, it could be demonstrated that stereoregular polypropylenes could also be obtained in solution. This opened the era of "single-site" catalysts.

The strong point of a homogeneous catalyst is its well-defined structure, which translates into a single active species and a corresponding microstructural uniformity of the polymerization products. Moreover, the active species can be designed – at least in principle – in order to achieve better/different catalytic properties. The drawback is that, for most industrial olefin polymerization process technologies, a heterogeneous catalyst is needed. Unfortunately, changing a homogeneous single-site catalyst into a heterogeneous (supported) one is a logical, but by no means simple, solution; in fact, it is the subject of this whole book.

1.2
Levels and Scales of Polymer Structure and Modification

Thermoplastic polyolefin polymers have reached a wide application range since their original introduction during the latter half of the 20th century. The adaptation to often quite difficult requirements to processability, mechanics, optics and long-term behavior has been achieved by a number of structural modifications, starting at the chain chemistry level and ending in the component design and processing step [1]. From a dimensional point of view this can be translated into a diagram for different (length) scales of polymer design (Figure 1.1). The following section of this chapter will deal with these levels as seen from the chemistry, the morphology, and the property sides of material design.

1.2.1
Chain Structure: Chemistry, Interaction, Regularity, and Disturbance

Polymer design starts at the level of the molecule, at the chain structure defining the basic characteristics of the material, such as being crystalline or amorphous, and thus determining application properties to a large extent. Polarity, ranging from apolar pure polyolefins to polycondensates with intensive hydrogen bridge formation between the chains, is one major factor here. While both polyamide-6 (PA-6, nylon) and HDPE have similar levels of crystallinity (~60%), their melting points are, at 220 and 135 °C, quite different. At the same time the reaction to

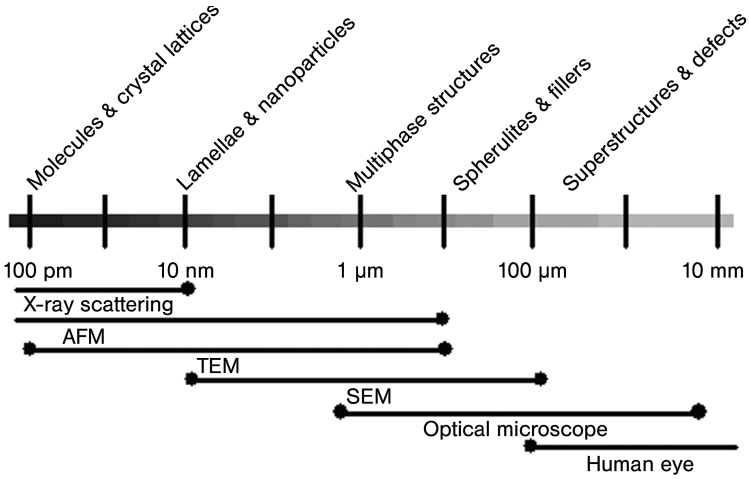

Figure 1.1 Structural levels and respective dimensions for the systematic modification of polymeric materials with appropriate investigation tools for characterization.

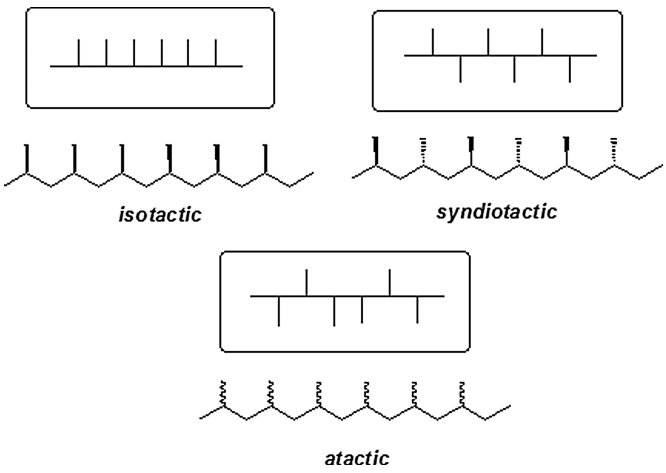

Figure 1.2 Tacticity.

environmental effects such as humidity and ultraviolet (UV) radiation will already be predetermined here. At a given level of polarity, stereochemistry and bulkiness of side groups has a decisive effect, separating crystallizable from amorphous subspecies of the same polymer; examples are the difference between atactic and isotactic polystyrene (aPS/iPS) or members of the polypropylene family – atactic (aPP), syndiotactic (sPP) and isotactic (iPP) [2] (Figure 1.2). Basically, the same effect – namely a disturbance of the chain structure first reducing and finally disrupting the ability to crystallize – can be achieved by copolymerization. One well-known point here is the crystallinity and density control of polyethylene (PE) by incorporating higher α-olefins such as 1-butene, 1-hexene or 1-octene, although

similar effects can also be achieved for aromatic polyesters with aliphatic diesters [3]. Further consequences of this modification, such as effects on melting temperature (i.e., sealing properties), crystal size (i.e., transparency), modulus (i.e., stiffness) and free volume (i.e., gas and vapor permeability) will be discussed below.

1.2.1.1 Chain Topology: SCB, LCB, and Special Structures

While stereostructure and chemistry suffice to describe the polymer chain at a local level of a few monomeric units, the chain topology is required to differentiate between purely linear and various branched polymers. The rheology and processability, but ultimately also the mechanical properties, of a polymer are decisively affected by the branching structure, which can be roughly split into short-chain branched (SCB) and long-chain branched (LCB) polymers [4]. The usual parameter serving as distinction here is the branch length or branch molecular weight, where LCB represents a branch molecular weight above the critical molecular weight (M_C) of the respective polymer. In detail, star-, H-, and comb structures must be differentiated, while the existence of "branches on branches" (also called "multi-branching", typical for low-density polyethylene, LDPE, from a high-pressure process [5]) adds a further dimension to the system's complexity (Figure 1.3).

1.2.1.1 Molecular Weight Distribution (MWD)

Technical polymers are polydisperse, showing a more or less broad MWD as result of a number of factors. Multi-site catalysts, kinetics and residence time distribution are among the main factors contributing to polydispersity, which can be related again to both processing and end-use properties, either directly or via the characteristic parameters of averages and moments (in the most simple case the number average, M_N, and weight average, M_W, molecular weight) [3, 6]. Two important distinctions must be made here: (i) the mechanical consequences of an MWD fraction are significantly higher (and the rheological ones lower) if the fraction is below M_C; and (ii) all changes are much more critical for glassy polymers, where

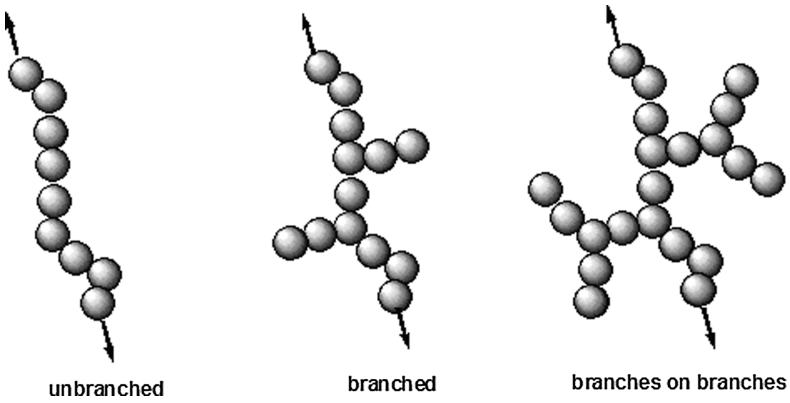

Figure 1.3 Schematic representation of chain topology.

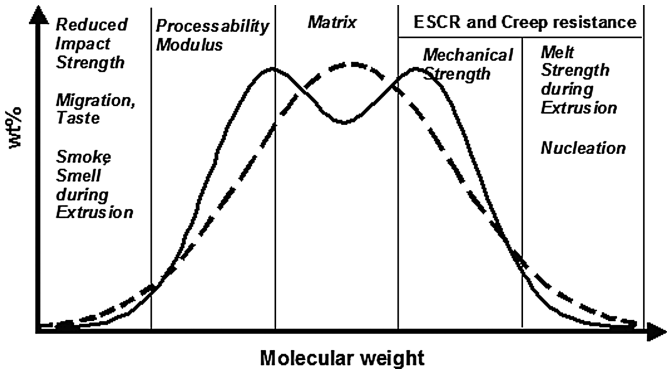

Figure 1.4 Contributions of various molecular-weight fractions to the property profile of polyethylenes with monomodal (dashed line) and bimodal (full line) molecular weight distribution.

the mechanics are defined by entanglements rather than by crystalline structures.

Modern polyolefin materials mostly have a rather elaborate designed MWD, in which the various fractions contribute to the different target properties (or problems) of the overall system. Figure 1.4 provides a rough outline of this property design for the case of bimodal polyethylenes, where this development is already well advanced, partly resulting from the very wide MWDs and possibly even with conventional Ziegler or chromium catalyst systems.

In reality, complete control of the produced MWD is limited by the characteristics of the catalyst and residence time distribution of the polymerization process. Chromium catalysts are unsuitable because of their inherently broad MWD, and even in the case of titanium-(Ziegler-)-catalysts limits are frequently reached in controlling the low-molecular-weight fraction (critical below M_C because of a lack of integration into the crystalline structure and entanglements) and extremely high-molecular-weight fractions (critical in film grades in which "gels" consisting of higher-molecular-weight or crosslinked material deteriorate the performance). A further limitation in broadening the MWD is the need to homogenize such materials, which also makes special extruder constructions necessary.

1.2.1.3 Blends and Other Multiphase Structures

As alloys are decisive for the wide application range of metals, blends and composites have further expanded the accessible property range of polymers. The underlying idea is to combine the advantages of different components, the base being a thermoplastic polymer, while the second (disperse) component can be inorganic (filler, fiber), elastomeric (and even crosslinked), or also thermoplastic [7, 8]. Details for these materials, which can be produced in multi-stage copolymerization, melt compounding or a combination of both processes, are provided below.

1.2.2
Semi-crystalline Polymers: From Lattices to Superstructures

Focusing the discussion on semicrystalline systems from now on is justified as this is the main area of catalytic and stereoselective polymerization. Even within this range of materials the variation in crystallinity, melting point and modulus is very wide and closely related to structural factors, as mentioned above.

1.2.2.1 Chain Structure and Crystallization Speed

The crystallization of polymers is a slow process in comparison to other materials such as metals. This results on the one hand from the high molecular weight and the related long characteristic times of the materials, and on the other hand from the low heat conductivity. It also limits the maximum degree of crystallinity, which for polyolefins rarely exceeds 60%. The process of solidification can therefore be separated into nucleation and crystal growth, which have been shown to be defined by different molecular characteristics of the polymer.

Crystal growth rate is defined mainly by the "smoothness" and regularity of the chain; consequently, among polyolefins the highest values are found for HDPE, which also has the most simple crystal structure based on chain folding (zig-zag structure in the lattice) only. Increased bulkiness will reduce the growth rate, as shown for a number of different polymers in Figure 1.5 [2, 9]. The maximum of the $G_C(T)$ function will normally be found approximately halfway between the melting point T_M and the glass transition point T_G, with PE being a notable exception. Polypropylene (PP) is one of the best investigated polymers in this respect, with both the contributions of stereoregularity and comonomer content being well documented [10]. A clear correlation to both processing speed and modulus can be recognized.

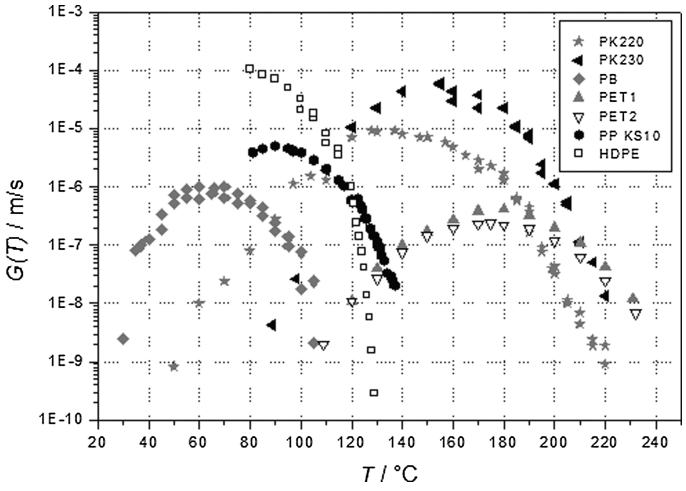

Figure 1.5 Temperature-dependence of crystal growth rate for polymers with different chain structure. (Data from Ref. [11].)

1.2.2.2 Lamellar Thickness and Modulus

A rather important contribution to the mechanical performance of polyolefins is the correlation of modulus to not only the overall crystallinity but also the lamellar thickness in the system. The latter is correlated to the crystallization temperature according to the Gibbs–Thompson equation (demonstrated for example for ethylene–octene copolymers by Rabiej et al. [12]), resulting in a general correlation also for the case of PP, as shown in Figure 1.6, where for three types of polymer-independent but parallel dependences were achieved. As shown in the report by Pukánszky et al. [13], although nucleation contributes significantly to the performance via this relationship, isotacticity effects [14] and also the isotactic sequence length are highly relevant.

1.2.2.3 Nucleation and Polymorphism

For the pure polymer the MWD and especially the high-molecular-weight fraction – that is, the part of the composition having the highest relaxation time and therefore acting as self-nucleants [15, 16] have been found to be decisive for the nucleation density ($N_C(T)$), which is the second decisive factor for mechanics and optics, but also shrinkage and warpage of injection-molded parts. The maximum of the temperature dependence of $N_C(T)$ is, however, located always at lower temperatures than $G_C(T)$, allowing the use of other highly efficient external nucleating agents as further design instruments. These are even more important for rather slowly crystallizing polymers such as syndiotactic PP. However, to be efficient, and especially to improve transparency, the efficiency must be rather high.

Special considerations must be taken in the case of polymorphic polymers such as isotactic and syndiotactic PP or poly-1-butene (PB-1). Normally, one of the

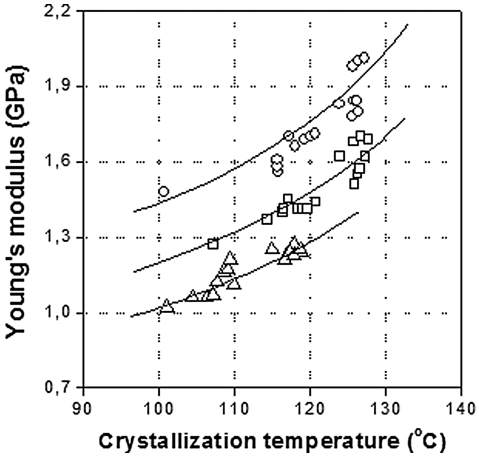

Figure 1.6 Dependence of the tensile modulus (Young's modulus) and crystallization temperature of non-nucleated and differently nucleated versions of three different polypropylene (PP) types: ○, homopolymer; □, impact copolymer; △, random copolymer. (Data from Ref. [13].)

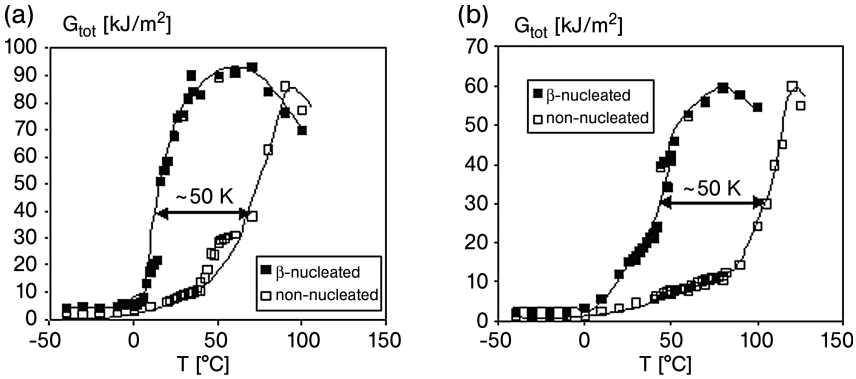

Figure 1.7 Evolution of the fracture energy, G_{tot}, with the temperature, T, for non-nucleated and β-nucleated resins with different flowabilities (melt flow ratios, MFR). (a) MFR 0.3 °C min^{-1}; (b) MFR 2 °C min^{-1}; a ductile-brittle transition temperature chosen as the temperature corresponding to half of the maximum of G_{tot} in the considered MFR range (this reflects the transition from a semi-ductile to a fully ductile behavior, without breaking the tested specimen). Test speed 1.5 m s^{-1} on injection-molded specimens. (Data from ref. [17].)

possible crystal modifications will be the most stable, being the α-modification for iPP. With selective nucleating agents the β-modification can be promoted in processing, resulting in materials with a significantly higher impact strength and allowing stretching into microporous films. The wide potential of these specifically nucleated iPP materials which also have a lower ductile–brittle transition temperature (see Figure 1.7) has been recently outlined in a review by Grein [17].

1.2.2.4 **Flow-induced Structures and Processing Effects**

Especially components and articles produced in conversion processes involving high deformation (shear or extension), such as injection molding, stretch-blow molding, mono- or biaxially oriented films or fibers, derive their morphology and application properties largely from flow-induced crystallization phenomena. These are well investigated for iPP, PB-1 and PE, and also demonstrate the strong influence of the MWD here. Notably, the group of Kornfield [18] has demonstrated the consequences of very small fractions of long molecules being related to the stronger orientation of these by flow stresses. Highly oriented skin layers with a far higher modulus than the less-oriented core of injection-molded specimens [19], as well as the enormous strength of highly oriented PE fibers, result from these mechanisms.

A similarly important role is played when quenching the normally semicrystalline polymers by very high cooling rates into materials with limited or even no crystallinity. Very drastic examples of this are poly(ethylene-terephthalate) (PET) and poly(lactic acid) (PLA), both of which can be quenched into a fully amorphous state. In the case of iPP, another crystal modification – the mesomorphic or smectic form – is achieved by quenching with cooling rates of more than 100 K s^{-1} [20]; this finding is of great practical relevance in the production of PP cast films.

1.2.3 Multiphase Structures

Blends and composites are considered whenever the highest mechanical requirements or seemingly conflicting property demands are confronted for a specific application. These need not be limited to mechanics, but can also involve dimensional stability or processability.

1.2.3.1 General Concepts of Impact Modification

Originally developed for the naturally more brittle amorphous polymers, the concept of elastomer-based impact modification is also applicable for semicrystalline polymers [21, 22]. The relevance is highest for polymers with a glass transition within the application temperature range, such as iPP ($T_G \sim 0\,°C$), adding mobility with elastomeric components having a far lower T_G, which is the case for ethylene-propylene-"rubbers" (EPR) in the range from –60 to –40 °C. Alternative concepts such as hard-phase impact modification with inorganic micro- or nanoparticles [23] have not yet gained widespread application, while crosslinked elastomer phases have a solid position for special areas.

1.2.3.2 Multi-stage Copolymers (PP)

While the addition of elastomeric impact modifiers such as EPR, ethylene propylene diene monomer (EPDM), styrene elastomers or ethylene-based plastomers in extrusion mixing allows for maximum flexibility in property design [7]; it also involves high cost, and the compatibility is often limited. The multi-stage copolymerization of propylene with ethylene (or higher α-olefins), where the elastomer is produced directly in the reactor, represents a much more economical way of producing materials with high impact strength. Products from the latter process are generally still called "block-copolymers", though a more correct name would be "heterophasic copolymers". In Figure 1.8, it can be seen that the polymer contains not only crystalline PP and essentially amorphous EPR, but also crystalline PE in the "core" of the EPR particles. The properties of these materials are defined by the quantity, size and internal structure of these soft particles, where the primary design parameter is the quantity of disperse elastomer phase. The linear effect on the modulus as compared to the step function in toughness is demonstrated graphically in Figure 1.6.

Further composition parameters such as molecular weight and comonomer distribution of the EPR phase allow reactor design [24], while the further addition of PE and other elastomer or filler components are used for post-polymerization modification.

1.2.3.3 Polymer Blends and Reactive Modification

Blends between polymers of different chemical nature, such as PP/PA-6 or PE/PS, almost always require compatibilization, for which either graft- or block-copolymers are applied [25]. Both, the combination of polar and non-polar property aspects (e.g., paintability with limited water uptake) and the possibility of reaching highest

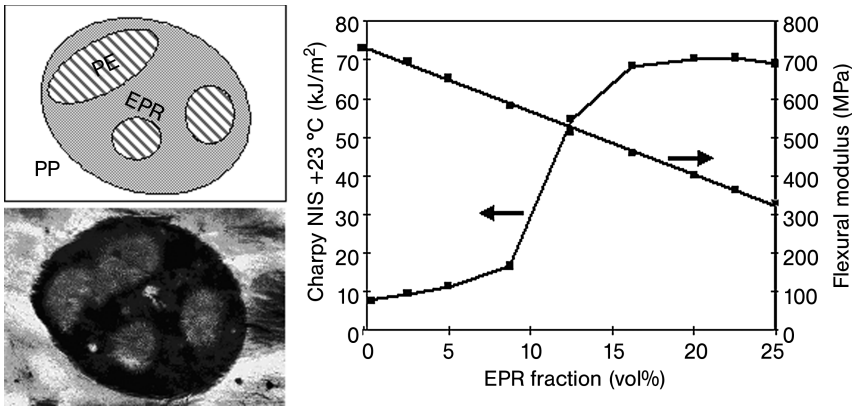

Figure 1.8 General structure of heterophasic EP-copolymers. Left: PP and PE crystalline, EPR amorphous; image from RuO_4-stained transmission electron microscopy image). Right: influence of the amount of elastomer phase (EPR) on stiffness and impact strength of such polymer systems.

temperature resistance by three-dimensional (3-D) network structures, as in glass fiber-reinforced PP/PA-6.

Special property combinations can be reached by reactive modification, which in the case of polyolefins is practically always based on radical grafting reactions [26]. The potential applications of this technology range from the production of long-chain branched PP with high melt strength offering advantages in foaming, and other processes with strong extensional flow, via the stabilization or partial crosslinking of phase structures (up to thermoplastic vulcanizates, TPVs) up to polar modifiers and compatibilizers (e.g., by grafting with maleic anhydride). In the case of PE the process is even more flexible because the inherent risk of degradation is lower.

1.2.3.4 **Compounds and (Nano)Composites**

Further modifications are possible, for example through the addition of fillers and reinforcements of mostly mineral nature. The possible mechanical profiles are determined by the properties of the base polymer, as well as by the quantity and nature of the filler [27]. Especially when using glass fibers, which open the highest strength level, further improvements are possible by modifying the fiber surface (sizing) and using compatibilizers (adhesives). Parts of this category are also organic reinforcing fibers from natural (regenerative) sources such as hemp, flax, or wood fibers. The strength of glass-fiber-reinforced materials is not achieved with such additions, and the lot-to-lot variations of natural fibers are problematic; however, the full combustibility of such composites is seen as an advantage.

The new generation of nanofillers promised even better opportunities for property profile optimization [28]. Very small and highly anisotropic particles resulting from an exfoliation of organically modified clay have a strong reinforcing potential

in polycondensates such as PA-6, whilst in polyolefins the problems of dispersion and exfoliation are much greater. *In-situ* methods are considered as a viable alternative here, as they avoid the problems of melt phase dispersion; however, they are still in the early stages of development for catalyst-based systems.

1.2.4
Property Optimization in Processing

One final possibility for optimizing part properties is the application of special processing (conversion) technologies. As mentioned above, the ultimate mechanical properties of semi-crystalline polymers depend heavily on not only the crystallinity but also the morphology of the formed crystalline structures. In this way, a massive increase in strength can be achieved through the targeted production of oriented structures; examples include the SCORIM (shear-controlled injection molding) process [29] or the "Push-Pull" injection-molding process. Even larger increases in the elastic modulus, and also in breaking strength, can be achieved in fiber-spinning processes by post-drawing in either the solid or semi-solid state. A combination of this process, with weaving and sintering of these high-strength PP-fibers to plates for later thermoforming, was developed by the group of Ward in the United Kingdom [30], and is presently marketed under the product name "curv". By using this technique, modulus values of up to 5000 MPa can be achieved.

1.3
Polymer Design: The Catalyst's Point of View

As illustrated above, designing polymer properties can be achieved at various scales. The following section concentrates on polymer design from a catalyst point of view. The primary role of a single-site catalyst is its ability to influence the molecular architecture of a polymer chain (molecular weight, MWD, comonomer incorporation and distribution, stereoselectivity, regioselectivity and block structure). Emphasis will be placed in this section on single-site α-olefin polymerization catalysts and their prodigious ability to tailor the molecular architecture of a polymer, through rational design of the steric and electronic environment of the active site. That said, however, it should be noted that the "true" rational design of a catalyst system is not commonplace, and the vast majority of reports of single-site catalysts have been more "pot-luck" than precision. Put in a nutshell, the art of single-site catalyst tailoring is the ability to encourage or discourage certain competing reactions, by tailoring the catalyst system, polymerization conditions (or both) to produce a polymer resin with a desired molecular architecture. The success of this approach has seen this fascinating area of catalysis and polymer science grow, in less than three decades, to truly gargantuan proportions. It has greatly benefited from the understanding of the kinetic mechanisms at play during polymerization, rational tailoring of the steric and electronic properties of the catalyst, activation, and the advent of powerful computational modeling. In addition,

the development of detailed physical measurements and rheological testing of the resultant polymer resins, facilitated by their narrowly dispersed nature that has allowed a synergistic combination of one or more of the above.

Due to the great volume of material, only the basic tools and concepts will be discussed here, along with illustrative "case studies". For a more detailed discussion, the reader is directed elsewhere [31–100].

1.3.1 Mechanisms and Kinetics: A "Tailors Toolbox"

At this point it is worth recapping on some of the basic developments in the understanding of metal-catalyzed polymerization processes. During a typical polymerization, numerous competing reactions are occurring with different rates and orders. Consequently, understanding the mechanisms and how their kinetic rates are affected by polymerization conditions – for example, are the rates monomer-dependent or independent? – can provide considerable help. Equally, an understanding of the steric and electronic requirements of a mechanism are important if the aim is to (potentially) raise or lower the energy of a transition state in order to promote or discourage a desired reaction, or to control how a monomer is enchained (stereo- or regioselectivity, etc).

1.3.1.1 Activation, Initiation, Propagation: On your Marks, Get Set, . . . Go!!

Activation The "activation" of a single-site precatalyst complex is typically achieved via contact with an appropriate cocatalyst species. It is crucially important to select the correct combination for the particular polymer process or target. It is also an area that is typically overlooked, with focus being paid to altering the complex rather than to the activation process. In terms of activity, major improvements can be achieved merely by altering the activation package.

Common procedures for generating "primary" ion-pairs start from metal chloride or alkyl precursors (Figure 1.9). For dichloride precatalysts (L-MCl_2), the generation of the species requires the initial conversion of one (L-M(R)Cl) or both of the chlorides (L-MR_2) into alkyls species. Subsequent abstraction of either the remaining chloride or the alkyl moiety forms a "primary" ion pair (cationic 14*e* metal center). Typically, although MAO fulfils all of the above criteria, they can also be achieved via a combination of alkylating agent and an abstracting agent (Cl or R). For dialkyl precatalysts, alkyl abstraction is typically achieved via two routes. Abstraction via Lewis acids such as $B(C_6F_5)_3$ or MAO is commonplace; however, ability of the resultant anions ($[RB(C_6F_5)_3]^-$ or [R-MAO]$^-$] to coordinate to the cationic metal center is heavily dependent on the nature of R and the ability to delocalize the negative charge in the cation. Alternate alkyl abstractors are Brønsted ($[HNMe_2Ph]^+$) or Lewis acidic ($[CPh_3]^+$) cations which contain a weakly coordinating counterion (e.g., $[B(C_6F_5)_4]^-$) [40–44].

It is important to highlight that formation of the "primary" ion pair is governed by kinetic considerations, and its chemistry is dominated by equilibria reactions,

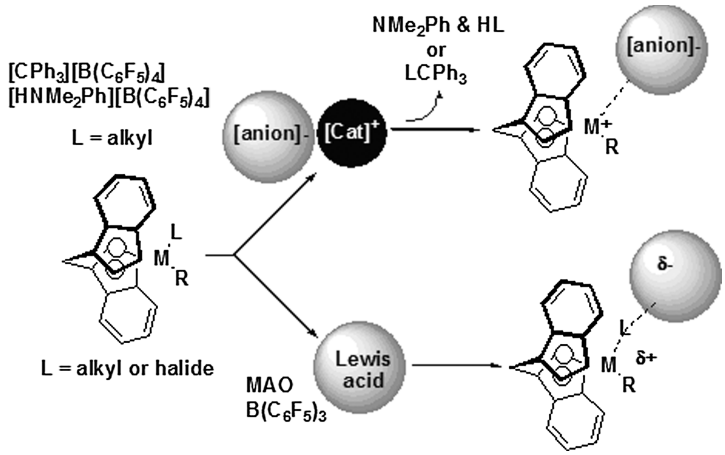

Figure 1.9 Schematic representation of precatalyst "activation" via archetypal Lewis and Brønsted acidic cocatalyst/activators.

for example the coordination of basic metal alkyls such as trimethylaluminum or even a dialkyl precatalyst complex to the cationic center.

Initiation The initiation of the polymerization process is believed to occur as a result of the displacement of the anion and coordination of the monomer in the "primary" complex. Whether the monomer binding is an associative or dissociative mechanism remains a matter of debate (Figure 1.10). Briefly, the anion dissociation mechanism generates an available coordination site on the metal center, which grabs a monomer for subsequent enchainment. Anion dissociation is an equilibrium reaction, and therefore the tendency for anion re-association would also arise. This begs the question of how fast the re-association reaction is, relative to the rate of propagation (does it interrupt the growth of a chain, or not?). The energetics of anion dissociation (charge separation) is also questionable in the non-polar environments that normally exist in industrial processes.

In the associative mechanism, monomer coordination and anion displacement is a concerted process. Therefore, how and in what direction the monomer approaches the metal center, and the steric influence of the anion may have important consequences for microstructure control [40–48].

As mentioned above, displacement of the anion and the coordination of the monomer are believed to result in the initiation of the active species, heralding the start of propagation. However, this still may not tell the whole picture, as interesting findings from the groups of Fink [49] and Landis [50] seem to suggest that the catalyst initiation step (active site formation) follows the irreversible insertion of the first monomer.

Propagation Once the active species is formed, the commonly accepted mechanism for chain propagation is based on the migratory insertion mechanism of

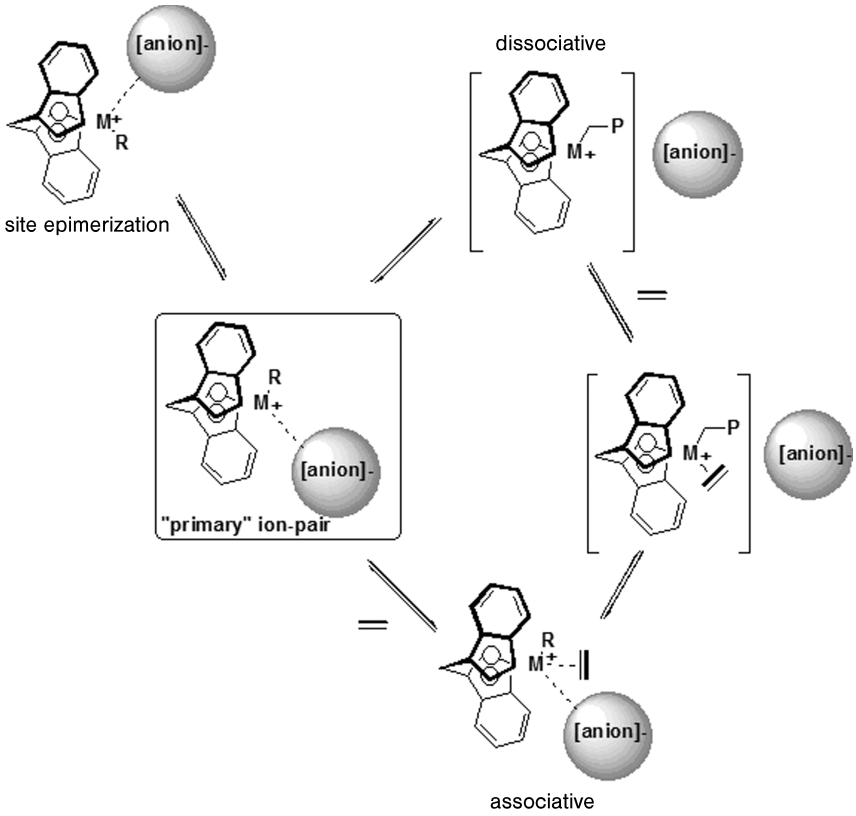

Figure 1.10 Schematic representations of associative and dissociative mechanisms for the coordination of an olefin.

Cosse–Arlman and further refinements [51]. The mechanism is basically a two-step process in which the olefin coordinates to the available coordination site metal center and is inserted via *cis* opening of the double bond, leading to chain migration (Figure 1.11; Site A to Site B). A regular alternation of insertions at the two coordination sites is expected under a kinetic quench regime; at the other limit, a Curtin–Hammett regime can be observed in case of fast (relative to insertion) relocation of the growing polymeryl between the two metal coordination sites (e.g., under conditions of monomer starvation). In addition, the mechanisms indicate that an olefin must be face-on to the metal, with the double bond parallel to the metal alkyl bond. The presence of α-agostic interaction "conformationally locks" the growing polymer chain and/or assists in stabilizing the transition state and secondary insertions, which may occur in α-olefins higher than ethylene; these are also illustrated in Figure 1.11 [52].

In very basic terms, the whole process up to this point is akin to a Formula 1 race. In the activation step, the driver (precatalyst) enters the car (cocatalyst) and switches the engine on. However, the race cannot start until the driver engages

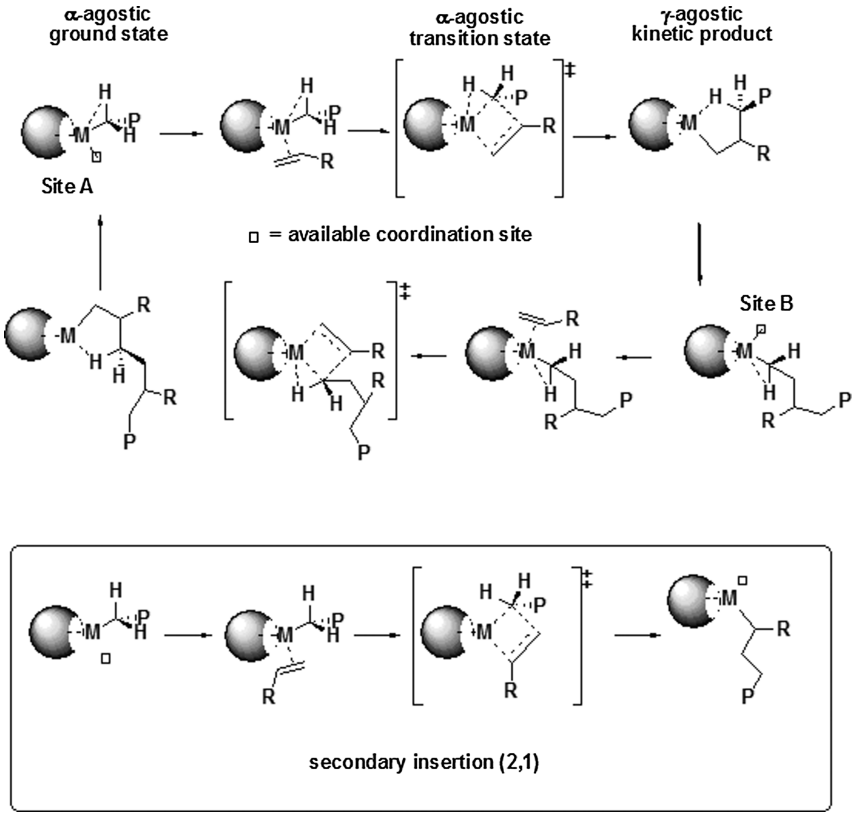

Figure 1.11 α-Agostic-assisted Cosse–Arlman mechanism (after Refs. [52a,b]).

the gear (coordinates olefin), drops the clutch (displaces the anion), and accelerates away (chain propagation).

1.3.1.2 Chain Transfer

Chain transfer is a statistical chain event in the life of a growing polymer chain. It is not necessarily the termination of the final polymer chain, as many chain-transferred products are subsequently reinserted. This is exemplified by the appearance of ethyl and methyl branches in the homo-polymerization of ethylene with metallocenes [53, 54], branch formation by the ubiquitous Brookhart systems [55], the formation of LCB polymers (vinyl released end-group macro-monomer re-insertion) [56], and reversible transmetallation ("chain shuttling") [57].

Understanding chain transfer can help in tailoring a catalyst's performance to either promote or discourage one or more of the chain-transfer mechanisms. Typically, tailoring starts by an analysis of the end-groups in a polymer produced by a "first-generation" system. The analysis of end-groups then provides a "fingerprint" of what types of chain transfer have occurred, and which are the dominant. "Second-generation" systems can then be designed to address any short comings

and to attain the desired molecular weight capabilities. Typically, two routes are employed to tune the molecular weight capabilities of a system: the polymerization conditions and the metal precatalyst. Investigations conducted by Fink and coworkers on ethylene insertion rates, into differing Ti–R bonds (rate of insertion R = Pr^n >> Et >> Me) may also be interesting to consider in terms of what group is left on the metal following chain transfer, and how quickly can that center reinitiate chain-propagation [49].

The apex of controlled chain transfer allows the formation of interesting block copolymers or polyolefins with extremely narrow molecular weight distributions ($M_w/M_n \approx 1.1$) [58]. The control of chain transfer can also allow the synthesis of resins with increased amounts of end-groups that are beneficial for post modification (e.g., crosslinking).

β-Transfer Chain transfer via β-hydride transfer occurs via two distinct mechanisms that afford a polymer chain with the same end-group: (i) β-hydride transfer to the metal center, yielding a metal hydride; or (ii) β-hydride transfer to an incoming (co)monomer, yielding a metal alkyl (Figure 1.12) [59–62]. β-Hydride transfer to a (co)monomer after a secondary insertion is also shown in Figure 1.12. Such a chain-transfer mechanism can become important in terms of molecular weight for such centers where propagation after secondary insertion is slow [59, 60, 63]. Whilst both mechanisms yield the same product, it is important to understand the difference and possible implications towards molecular weight tailoring.

β-Hydride transfer to metal is a unimolecular process, and the transfer rate is independent of monomer concentration. For most systems, the propagation is dependent on monomer concentration, and therefore an increased monomer concentration can lead to high molecular weights. In contrast, β-hydride transfer to a (co)monomer is dependent on the monomer concentration, and therefore increases proportionally with the propagation rate; as a result, the molecular weight is often

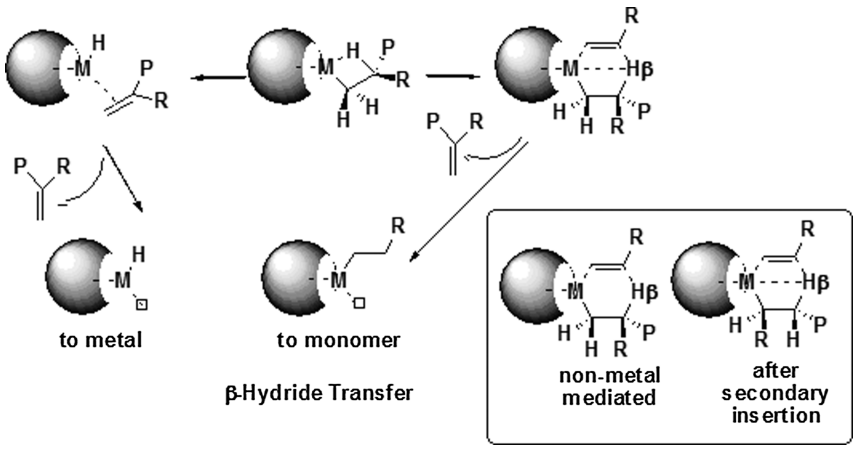

Figure 1.12 Schematic representations of β-hydride chain-transfer reactions.

independent of the monomer concentration. Generally, speaking β-hydride transfer to a (co)comonomer is the dominant termination mechanism.

A variety of end-groups results from β-hydride transfer to a (co)comonomer, and these are dictated by what and how the last (co)monomer was enchained (ethylene or 1-olefin; primary or secondary insertion). For primary insertion, β-hydride transfer leads to the formation of a vinyl (ethylene; CH_2=CH_2-polymeryl) or vinylidene (1-olefin; CH_2=CH(R)-polymeryl) polymer end-group. In contrast, *trans*-vinylene end-groups arise following β-hydride transfer following a secondary insertion of propylene or a higher α-olefin.

β-Me transfer to the metal center is an additional chain-transfer mechanism in propylene polymerizations. As shown in Figure 1.13, such a termination mechanism results in a vinyl end-group for propylene, forming a potential macromonomer (LCB) [64], unlike the vinylidene product from a β-hydride-transferred chain transfer [65].

Chain-transfer Agents: Transmetallation and Hydrogenolysis Chain transfer via transmetallation occurs through a metal alkyl-containing chain-transfer agent, via an exchange of the polymer chain and the chain transfer agent's alkyl group. Such chain-transfer agents are typically, but necessarily, aluminum alkyl compounds such as Al_2Me_3 or Al_2Et_3. Following termination and work-up of the resultant polymer resin, the reactive Al–carbon bonds are hydrolyzed to yield a saturated hydrocarbon (Figure 1.14). However, chains residing on aluminum can be

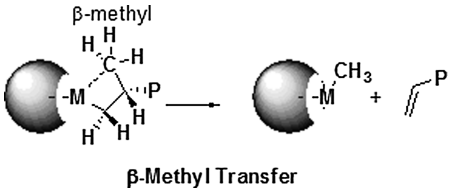

Figure 1.13 Schematic representations of the β-methyl chain-transfer reactions.

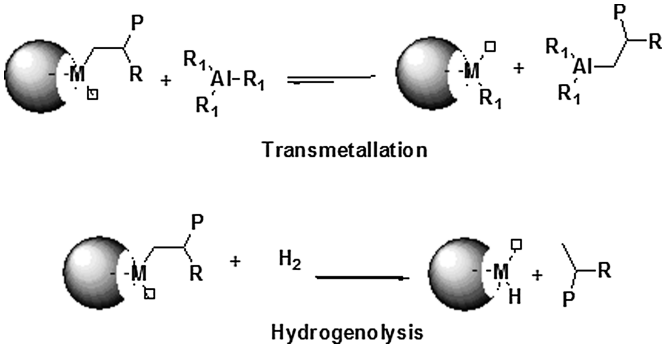

Figure 1.14 Schematic representations of transmetallation and hydrogenolysis chain-transfer reactions.

captured and converted into useful macromonomers [66]. It should be noted that this reaction is reversible – that is, the secondary metal can transfer this chain back to an active site. Mastering this reaction has resulted in a recent major breakthrough in polyolefin catalysis, and this will be discussed in more detail in a subsequent section [57].

Chain transfer via hydrogenolysis is achieved by the addition of hydrogen, which leads to saturated end-groups (Figure 1.14). As hydrogenolysis is the preferred means of controlling the molecular weight under industrial conditions, an understanding of how reactive a catalyst system is to hydrogen, and how it affects productivity, is extremely important in any catalyst system, particularly for the single-site catalysts which are commonly highly reactive towards hydrogen.

1.3.1.3 **Insertion Control**

Copolymerization Control Ethylene copolymers (e.g., ULDPE, VLDPE, LLDPE, MDPE) represent the most successful application area of single-site catalysts. The control of such copolymerization is primarily achieved through an understanding of the relative reactivity ratios of ethylene and comonomer(s) for a particular system (precatalyst + cocatalyst).

Ethylene is the most reactive olefin, with alpha-olefin reactivities decreasing as the length of the alkyl group increases. However, the rate of decrease in the reactivity diminishes as the length of the alkyl group increases. Linear α-olefins are more reactive than their branched counterparts, with a drastic decrease in reactivity seen for the branched molecules at the β-carbon (CH_2=CRR′). This effect is generally attributed to steric crowding in the vicinity of the reactive double bond.

Apart from the general reactivities of α-olefins, their reactivity is highly dependent on the catalyst structure [67]. In general, single-site catalyst are more reactive towards α-olefin comonomers than are traditional catalysts (e.g., Ziegler and Cr), although the reactivity of an α-olefin is highly dependent on the metal and the ligand structure. Electronic factors at the active site, as well as steric environment in the vicinity of the active site, determine the reactivity and structure of the copolymer (SCB, M_w). Although many general conclusions on the influence of ligand structure on polymer structure have been drawn, the details of how the combination of electronic and steric affects the relative reactivities remain unclear. Ligand substitution, active metal and the presence of some form of rigidity in the structure (e.g., *ansa*-bridges) each have distinct effects on the polymerization behavior [68].

Stereo-regio Control A prochiral α-olefin molecule can insert into a M–R bond in four different ways, depending on the regiochemistry (1,2 or 2,1), and on the choice of the enantioface (*re* or *si*). In most cases, a strong preference is observed for one insertion regiochemistry (usually the 1,2); compared with heterogeneous Ziegler–Natta catalysts, however, most homogeneous single-site catalysts (and particularly metallocenes) are remarkably less regioselective, and occasional regio-

defects are detected in the polymer by using ^{13}C NMR, these typically being in the form of head-to-head/tail-to-tail enchainments.

The stereochemistry of a polymerization reaction is governed by the symmetry and steric environment of the metal center (ancillary ligand and anion) and the growing polymer chain. In the latter case, the stereogenic center formed by the last monomer enchainment influences the stereochemistry of the subsequent monomer addition. If this influence is significant and overrides that of the ancillary ligand, then the stereochemical regulation of the process is referred to as "chain-end-controlled". The archetypal examples of this are isotactic enriched polypropylene from low-temperature polymerization with Cp_2TiPh_2 (primary insertion) [69] and syndiotactic polypropylene from vanadium-based Ziegler catalysts (secondary insertion) [70]. If the single-site catalyst contains a chiral ancillary ligand set that is able to induce a "chiral pocket" at the active site, and which overrides the influences of the polymer-chain end, then the stereochemical regulation of the process is referred to as "enantiomorphic-site-controlled". It is this process that is most amenable for the rational tailoring of a catalyst and, subsequently, the polymer microstructure that is formed.

Enantiomorphic Site Control In the majority of cases, enantiomorphic site control can be predicted by the symmetry of the metal center. Ewen was the first to link the symmetry at a metallocene center and the microstructure of the resultant polymer (Figure 1.15) [71]. Strictly speaking, the active species is asymmetric due to the presence of the growing polymer chain and the available coordination site; however, it is assumed that the polymerization rapidly equilibrates between the

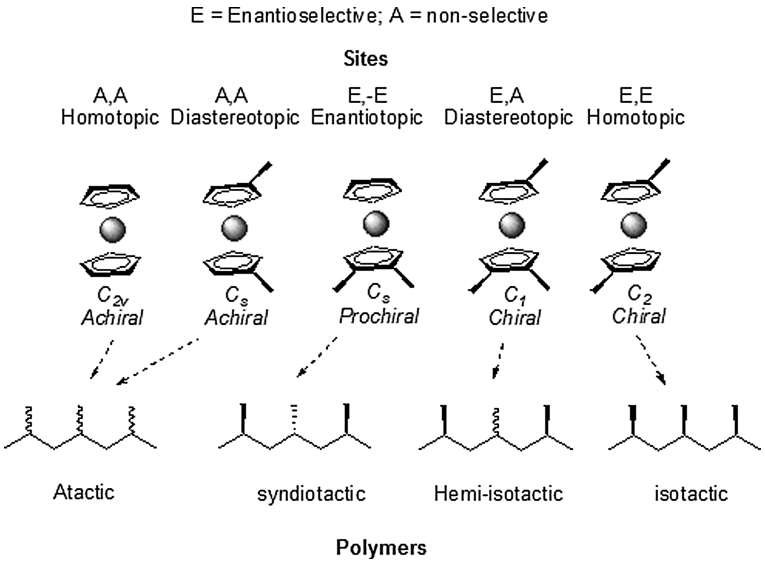

Figure 1.15 Ewen's symmetry rules.

two coordination sites. Based on Ewen's symmetry rules, the catalysts are divided into five main symmetry categories [71]:

- C_{2v} symmetric catalysts typically produce atactic or moderately stereoregular polymers (chain-end-controlled).
- C_s symmetric catalysts containing two distereotopic coordination sites typically produce atactic or moderately stereoregular polymers (chain-end-controlled).
- C_s symmetric catalysts containing two enantiomorphic coordination sites frequently produce syndiotactic polymers.
- C_1 symmetric catalysts are distereotopic and contain an enantioselective and non-selective coordination site. Ewen's symmetry rule predict a hemi-isotactic structure where alternating chiral–achiral insertion takes place. In practice, however, balancing the "steric excesses" is very important and makes prediction based only on symmetry very difficult.
- C_2 symmetric catalysts contain two homotopic sites and typically form isotactic polymers via enantiomorphic site control (both racemic and enantiomerically pure versions).

Although the Ewen symmetry rules are rather simplistic, they are typically the first starting point for catalyst design. Tailoring of the catalyst then revolves around the ability to dictate in which direction the growing chain is orientated, and how the incoming monomer is presented by the application of "steric pressure" (repulsive non-bonded interactions). Detailed mechanistic studies concerning enantiofacial selectivity, α-agostic-assisted olefin insertion and their relevance to stereocontrol, as well as the possible role that anions play, may be found elsewhere [59–62].

Defects The stereocontrol of a polymerization reaction, as with most things in life, is not perfect. Defects are enchained (stereo-error or regio-error) into a polymer during its lifetime, and occur, typically, via either the mis-insertion of a monomer or following an epimerization reaction (site or chain). As the frequency and distribution of defects plays a key role in dictating the polymer's properties, an understanding of how they arise and what they are dependent on has become a key feature in catalyst design.

In isotactic polypropylene polymerization there are two main types of chain defect, regio-error or stereo-error (Figure 1.16). The mechanism shown in Figure 1.17 is the idealized enantiomorphic site-controlled enchainment of propylene. As can be seen, the growing monomer chain is orientated in such a way as to minimize the non-bond interaction with the benzo-fragment of the indenyl moiety. In addition, the incoming ligand is enantiofacially presented in such a way as to minimize any interaction with the growing chain. The combination of homotopic sites, the controlled orientation of the growing chain, a consistent presentation of the correct enantioface of monomer, and an absence of chain-end epimerization, leads to the formation of pure isotactic polypropylene.

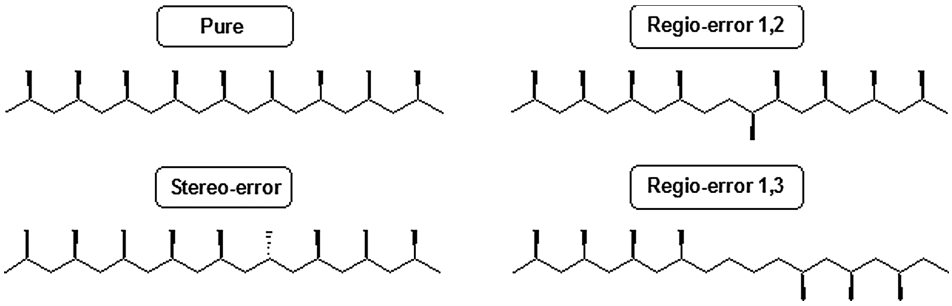

Figure 1.16 Stereo- and regio-defects in isotactic polypropylene.

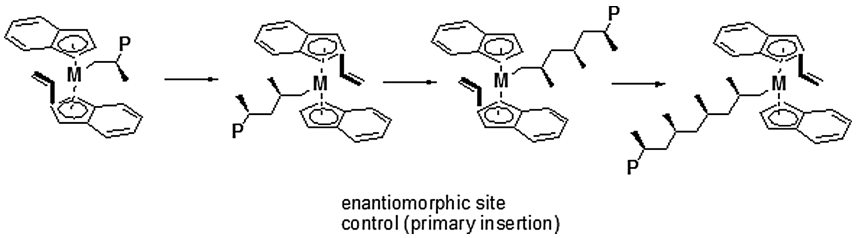

Figure 1.17 Schematic representation of chain propagation on a C_2 symmetric catalyst via enantiomorphic site control.

Figures 1.18 and 1.19 illustrate the various mechanisms that have been proposed to account for stereo-defects (Figure 1.18) and regio-defects (Figure 1.19) in isotactic polypropylene catalyzed via C_2-symmetric systems. Stereo-errors are thought to result from the enchainment of a propylene monomer with the "wrong" enantioface, or via a unimolecular chain-end epimerization mechanism. The latter mechanism is thought by some to be the dominant cause of stereo-defects due to the fact that such defects tend to increase with decreasing monomer concentration (lower propagation rates but the same chain-end epimerization rate). Regio-errors result from a secondary insertion of propylene; if this secondary insertion is propagated, then a 2,1-regio-defect is formed. However, if propagation after a secondary insertion is slow relative to a chain-end epimerization reaction from a secondary to a primary alkyl (alleviating steric hindrance), then a 1,3 regio-defect is formed.

Defects (stereo- or regio-errors) in the backbone of an isotactic polypropylene disrupt the chain in a similar way that the addition of comonomer does in polyethylene or polypropylene (EPR). As discussed above, chain disruption affects the crystallization parameters of the polymer and, in turn, some of its physical properties. Assigning the impact of one type of defect compared to another is a matter for debate; it would appear from Figure 1.16 that the 2,1 and 1,3 regio-error defects seem to have a larger defect foot-print (more disruption of the chain) than the stereo-error defects. Fischer and Mülhaupt, however, clearly proved that both regio- and stereo-error units are incompatible with the crystal lattice. Moreover,

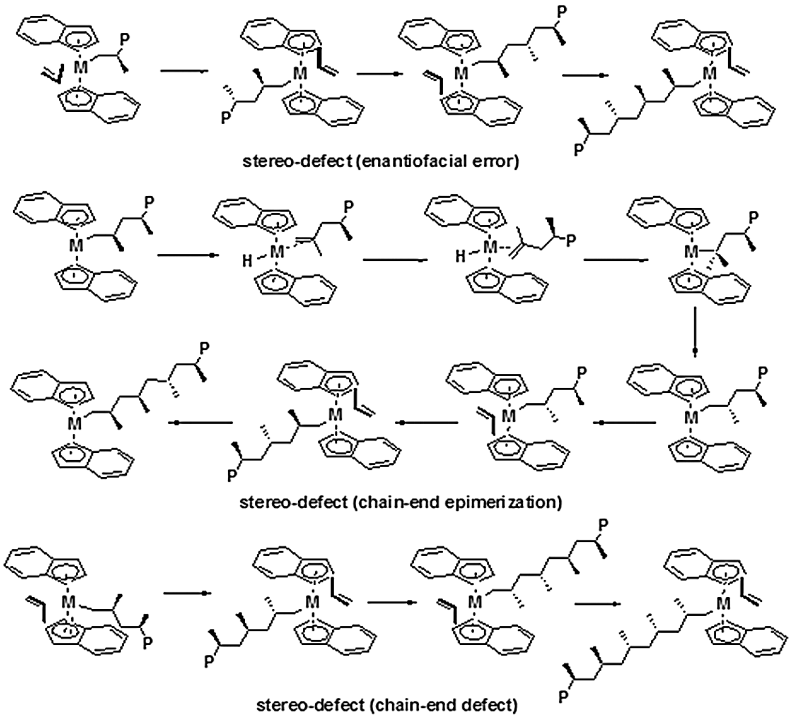

Figure 1.18 Stereo-defect formation.

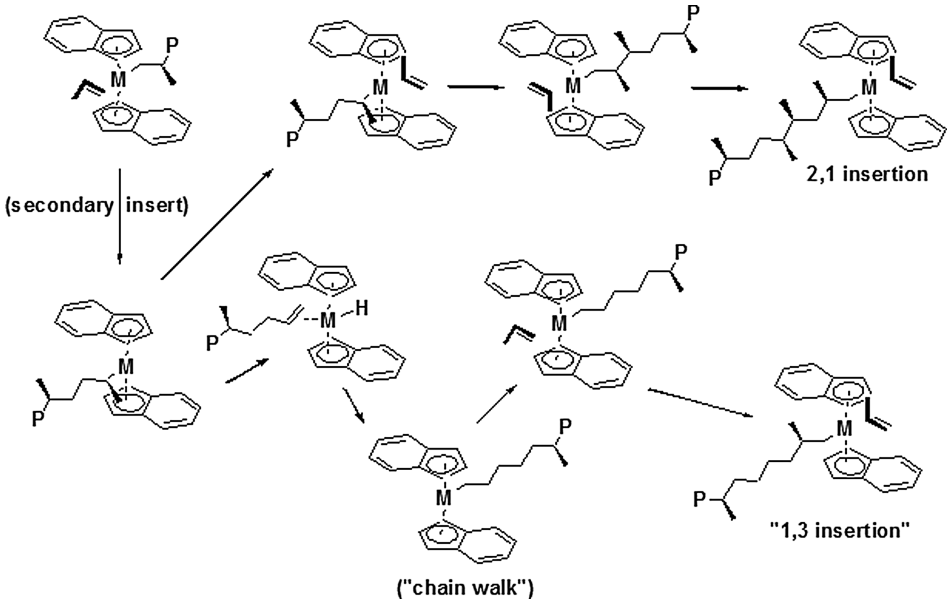

Figure 1.19 Regio-defect formation.

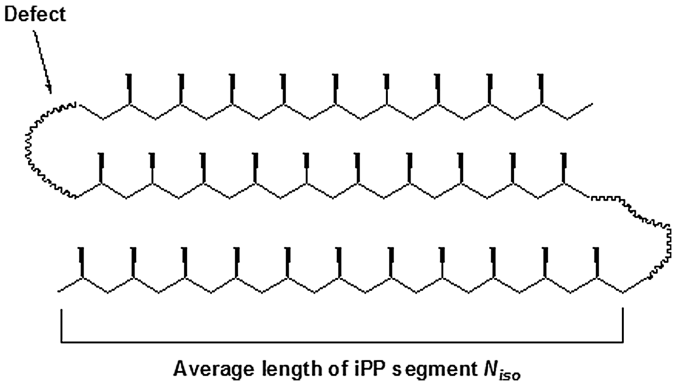

Figure 1.20 Schematic representation of the average length of iPP sequences.

the key to the situation is the distribution of defects and, more importantly, the average pure isotactic segment length (crystallizable sequence) between defects (n_{iso}) (Figure 1.20) [72a]. As might be imagined, the molecular weight of the polymer (M_w) and the number of defects need also to be taken into account.

Single-site catalysts typically distribute their defects homogeneously throughout the length of a polymer chain, unlike Ziegler–Natta catalysts which tend to "concentrate" defects in blocks with extremely long isotactic segment lengths. As a result, the more homogeneous a distribution, the more effective it is in segmenting the polymer (for the same molecular weight and defect content). Single-site catalysts typically have short isotactic segments (n_{iso}), and as a result they commonly crystallize in the γ-form (the γ-form modification of iPP is often achieved by the incorporation of low amounts of comonomer, typically ethylene), which has implications for certain, notably optical, properties (the γ-form does not form spherulites). The relevance of isotactic sequence length – especially for highly isotactic polypropylenes – to the achieved modulus level has been demonstrated by Viville et al., by utilizing a combination of analytical methods [72b]. It should always be remembered, however, that a variety of factors in combination play a role in defining the properties of microstructure, molecular weight, molecular weight distribution, and morphology of the crystalline domains. A more homogeneous distribution of regio-errors also has implications for propylene copolymers (in particular of ethylene copolymers), as ethylene is thought to be much more effective at insertion following a secondary insertion of propylene. This leads to a more random distribution of comonomer in the case of single-site catalysts.

Stereo-defects arise in syndiotactic polypropylene derived from the Ewen/Razavi family of C_s symmetrical metallocene (Figure 1.21) [73]. As described above, an enantioface error and a chain-end-epimerization lead to the propagation of a stereo-defect. However, as the C_s symmetric metallocene has a distereotropic site, a site-epimerization reaction ("back-skipping") can result in the formation of the same enantiomeric site. Hence, rather than alternating between the distereotropic sites, two consecutive insertions occur at the same enantioface, a process which

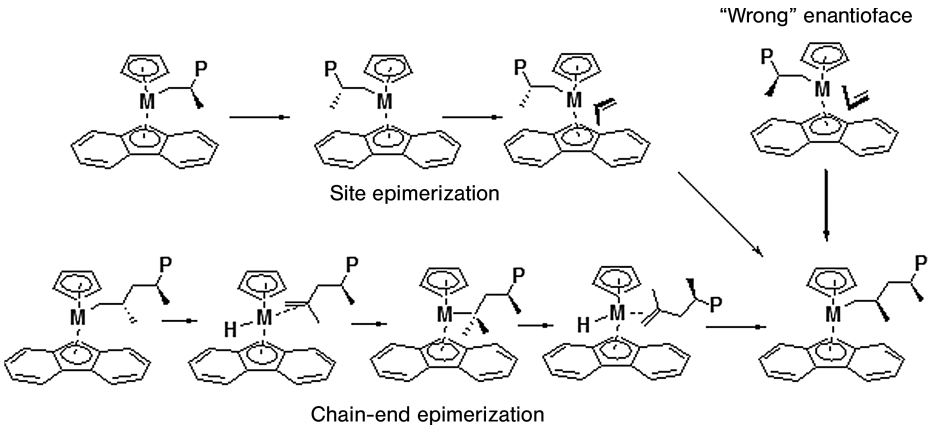

Figure 1.21 Schematic representation of stereo-defect formation on a C_s symmetric catalyst.

is possibly anion-assisted (Figure 1.22) [45]. Site epimerization does not result in stereo-defects in C_2-symmetric complexes, as their sites are homotopic and therefore site epimerization forms the same enantioface.

1.3.1.4 Summary

This section has hopefully illustrated the range of mechanistic tools that can be used to tailor the behavior of a precatalyst. One of the most important points to note is that migratory insertion requires the active metal center to possess at least two active sites. The nature of each active site is determined by the metal and the steric, electronic nature and symmetry that the ancillary ligand imparts to the metal, as well as the cocatalyst. It is also influenced the structure of the growing chain arising from various insertion (primary or secondary *re* or *si*). Therefore, a "single-site" catalyst can in fact possess numerous active sites with differing reactivity ratios to (co)monomer or chain-transfer agents, different regioselectivity and enantioface stereoselectivity. However, under set conditions the above processes behave, statistically, in the same way from one polymer chain to the next.

1.3.2 Case Study 1: Development of Commercially Relevant Single-Site iPP Catalysts

The development of commercially relevant single-site iPP catalysts is perhaps the archetypal elegant example of what the rational tailoring of a precatalyst can achieve, in terms of activity and the polymer resins that they produce.

The genesis of commercial single-site iPP catalysts and their development can be traced back to the stereo-rigid C_2-symmetric metallocenes of Brintzinger (*rac*-Et(Ind)MCl_2, M = Ti or Zr) [74]. It was Ewen, whilst employing the titanium catalyst above, who first correlated the C_2 symmetry of the metallocene to isotacticity [75]. However, the titanium complex proved too thermally unstable and had a low isotacticity. By using the zirconium analogue, Kaminsky and Brintzinger attained

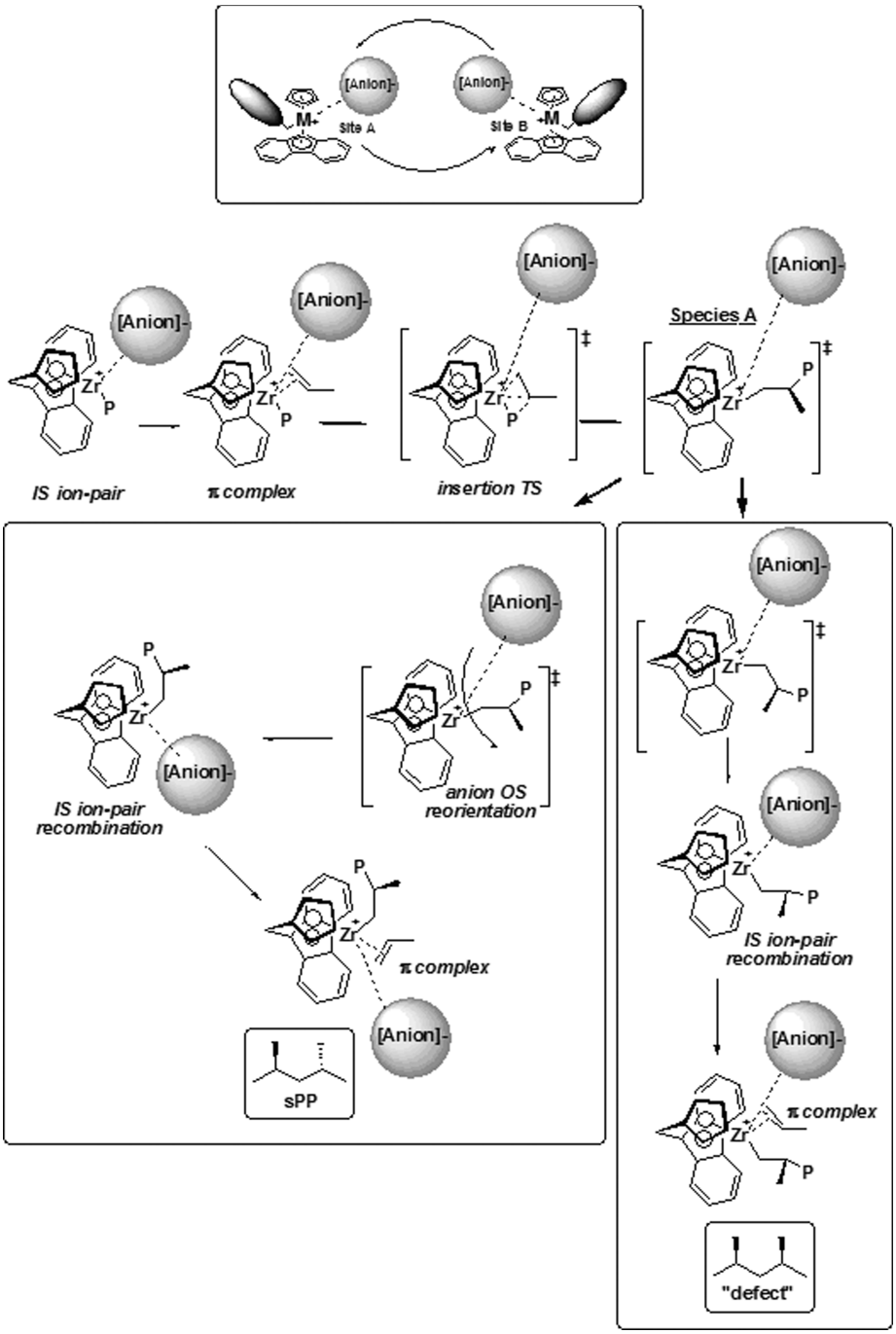

Figure 1.22 Site epimerization.

higher thermal stabilities and stereoselectivities [76]. Subsequent development of the bridged bis-indenyl zirconocenes indicated that the nature of the bridging atom could increase the stereoselectivity and molecular weight of a polypropylene ($H_2C < Me_2 < C_2H_4 < Me_2Si$) under industrially applicable conditions, although all of these systems were far from being commercially viable catalysts (Figure 1.23) [60].

Ultimately, it was the seminal studies of Spaleck and coworkers, with their rational tailoring of the basic C_2-symmetrical complex $Me_2Si(Ind)ZrCl_2$ (C_2-1) (Figure 1.24; Table 1.1) which truly illustrated the full potential [77]. As can be seen from Figure 1.24 and Table 1.1, the introduction of a methyl group in the 2 position of the indenyl moiety increased the molecular weight and stereoregularity, and was also found to reduce region-errors. The result was the production of polypropylenes with higher melting points, albeit with reduced activity. The introduction of an aryl ring in the 4-position of the indenyl moiety increased the polymer's stereoregularity, but once again a reduction in activity was observed. Finally,

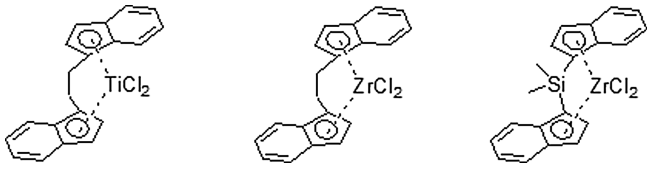

Figure 1.23 Evolution of C_2-symmetric complexes for the isotactic polymerization of propylene.

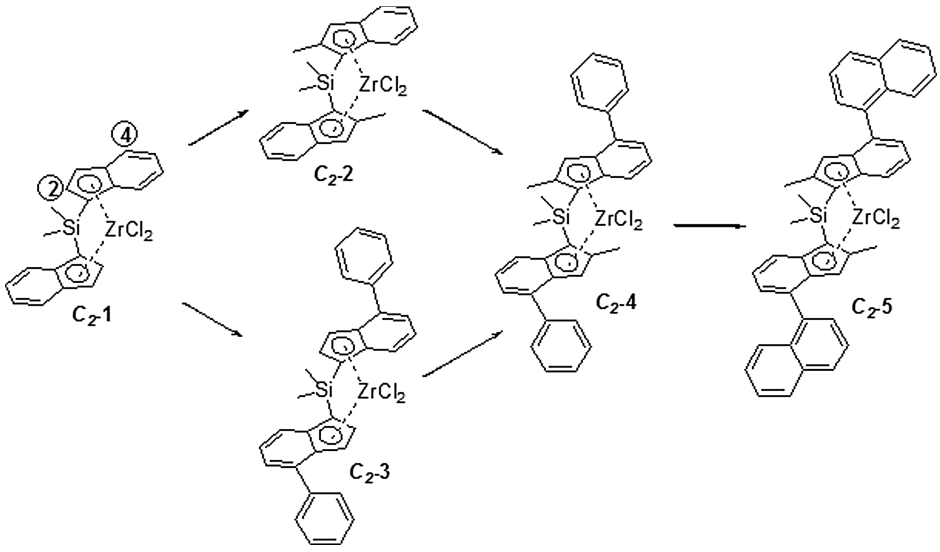

Figure 1.24 Evolution of a C_2-symmetric catalyst.

Table 1.1 Polymerization performances of Spaleck and coworkers C_2 symmetric complexes [77].

rac-Zirconocenes	***C_2-1***	***C_2-2***	***C_2-3***	***C_2-4***	***C_2-5***
Activity (kg PP $mmol_{Zr}^{-1} h^{-1}$)	190	99	48	755	875
% *mmmm*	81.7	88.5	86.5	95.2	99.1
T_m	137	145	148	157	161
M_v	36 000	195 000	42 000	729 000	920 000

a combination of substituents in the 2 and 4 positions of the indenyl moiety led to an order of magnitude increase in activity, along with increased stereoregularity, molecular weight and melting point of the final polymer resin.

Further evolutions of "Spaleck-type" polypropylene catalysis has led to catalysts with reportedly increased activities, molecular weights, and melting points. Such development has also further refined the structures [78], and highlighted the importance of the bridging atom and the substituents on it [79], as well as the active metal center [80]. In addition, it has heralded the development of the heterocene-based systems of Ewen, Jones and Elder, which have added yet another dimension to the "tailors toolbox" (not only for polypropylene) [81, 82]. Interestingly, similar structure–property relationships can be seen in ethylene-1-octene polymerization with C_2-1, C_2-2, C_2-4, C_2-5. Mülhaupt and coworkers reported that substitution in the 2 position of the indenyl moiety leads to increased molecular weights, while the addition of an aryl functionality in the 4 position increased the ability to incorporate comonomer [83]. Once again, the combination of these two changes led to a considerable increase in molecular weight and activity for a given comonomer incorporation (density).

The effect of the steric influence on molecular weight capability and stereoselectivity is easily understood. From a stereoselectivity point of view, the introduction of aryl and methyl groups allows for a better orientation of the growing polymer chain. As for molecular weight, if we consider the steric requirements for the transition states for chain propagation and chain transfer via β-hydride transfer to monomer (see Figure 1.11), a rather compact, four-centered transition state is seen to be required for chain propagation, and this can be accommodated in a relatively small space. Chain transfer to the (co)monomer, on the other hand, requires a six-centered transition state (see Figure 1.12) which utilizes more space and is more likely to be destabilized by the steric hindrance of the ligand framework. The increase in activity can be rationalized by the effective separation of the electrophilic active center and the counterion induced by the steric environment induced by the ligand, which in addition may hinder dinuclear deactivation mechanisms. The substitution pattern potentially enhances the degree of unsaturation associated with the active cationic center, thus increasing the reactivity towards propylene. The culmination of these studies led to the first single-site polypropylene catalysts with commercially viable performances.

1.3.3
Case Study 2: One Monomer, Many Microstructures

1.3.3.1 Propylene

The impact of what may seem like "subtle" changes in the stereochemistry and steric environment of the catalyst may have a considerable impact on the microstructure of the polymer [73, 84–87]. The different polypropylene microstructures, ranging from syndio, isotactic to atactic, that can be obtained by slight variations in the ligand environment are highlighted in Figure 1.25. The figures also illustrates how finely balanced some systems are; like a modern-day fighter aircraft, they are extremely agile and capable of an extraordinary range of "maneuvers" but more often than not this agility is based on an inherent "instability".

Although complex *Cs*-2 possesses all the symmetry and structural requirements of a syndio-specific catalyst, when activated this catalyst produces perfectly atactic polypropylene. The dynamic interchange between pseudo-axial/equatorial C–H (boat/chair confirmation on either side) geometries is presumed to disrupt the balance of steric forces and stereorigidity (Figure 1.26) [87].

The delicacy required when balancing steric control is highlighted by the C_1-symmetric family of metallocenes. From Ewen's symmetry rules, the predicted microstructure should be hemi-isotactic, but a range of polymer microstructures can be obtained depending on the "steric excess" of the substituent on the 3-position of the cyclopentadienyl moiety. Complex C_1-1 [84] is capable of producing hemi-isotactic polypropylene, whilst C_1-2 [85] and C_1-3 [86] have been used to prepare iPP or hemi-isotactic stereo-block polypropylene, respectively.

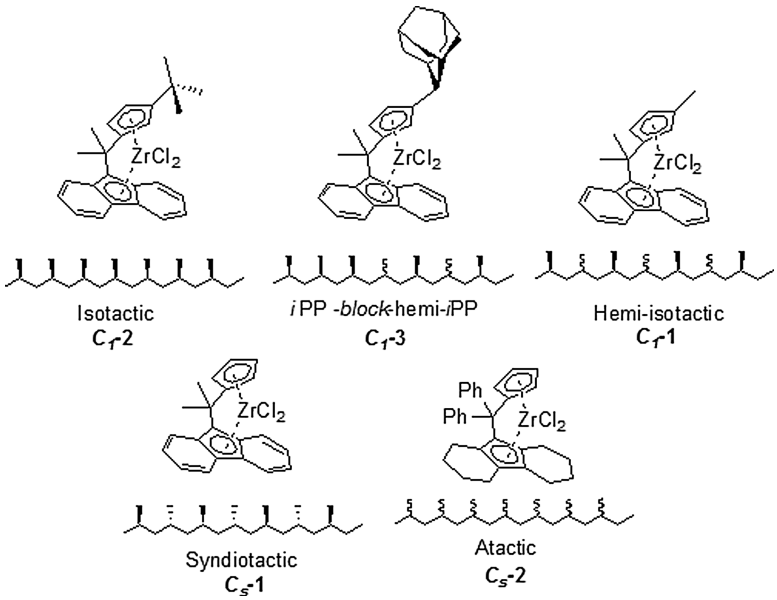

Figure 1.25 Symmetry is just part of the puzzle.

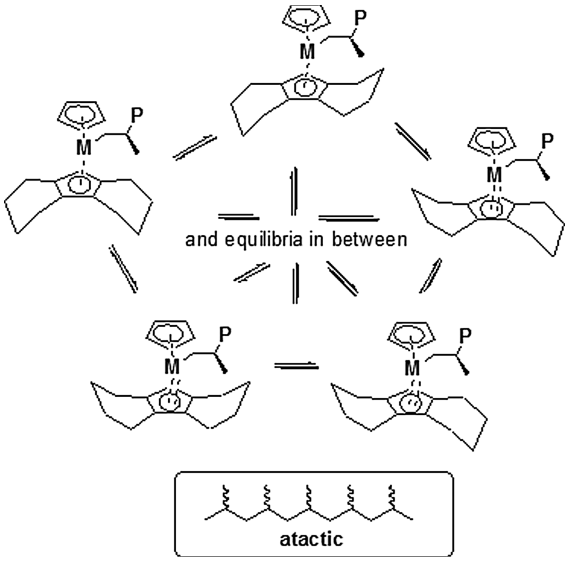

Figure 1.26 A mechanism for the formation of atactic polypropylene from a C_s symmetric catalyst.

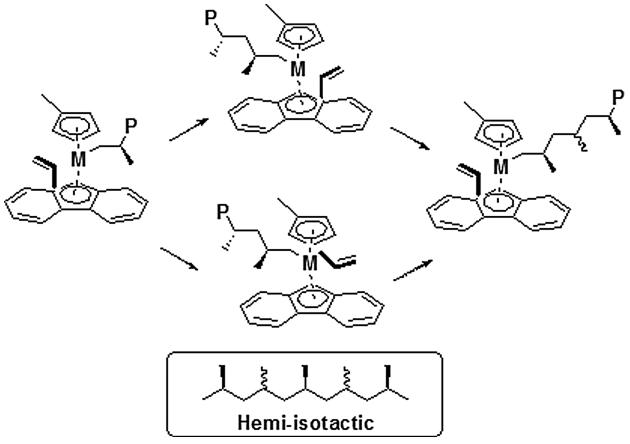

Figure 1.27 Formation of hemi-isotactic polypropylene.

The formation of hemi-isotactic PP is best explained via typical migratory insertion with distereotopic sites, one of which is enantioselective and the other aselective (Figure 1.27). The formation of isotactic or hemi-isotactic stereo-block polypropylene remains a topic for debate. At present, two limiting mechanisms are proposed for the formation of isotactic polypropylene. These are "site epimerization" or "alternating" mechanisms (Figure 1.28). The prevailing literature has invoked the "site epimerization" mechanism to explain the formation whereby, following migratory insertion at the enantioselective site (Site B in Figure 1.28),

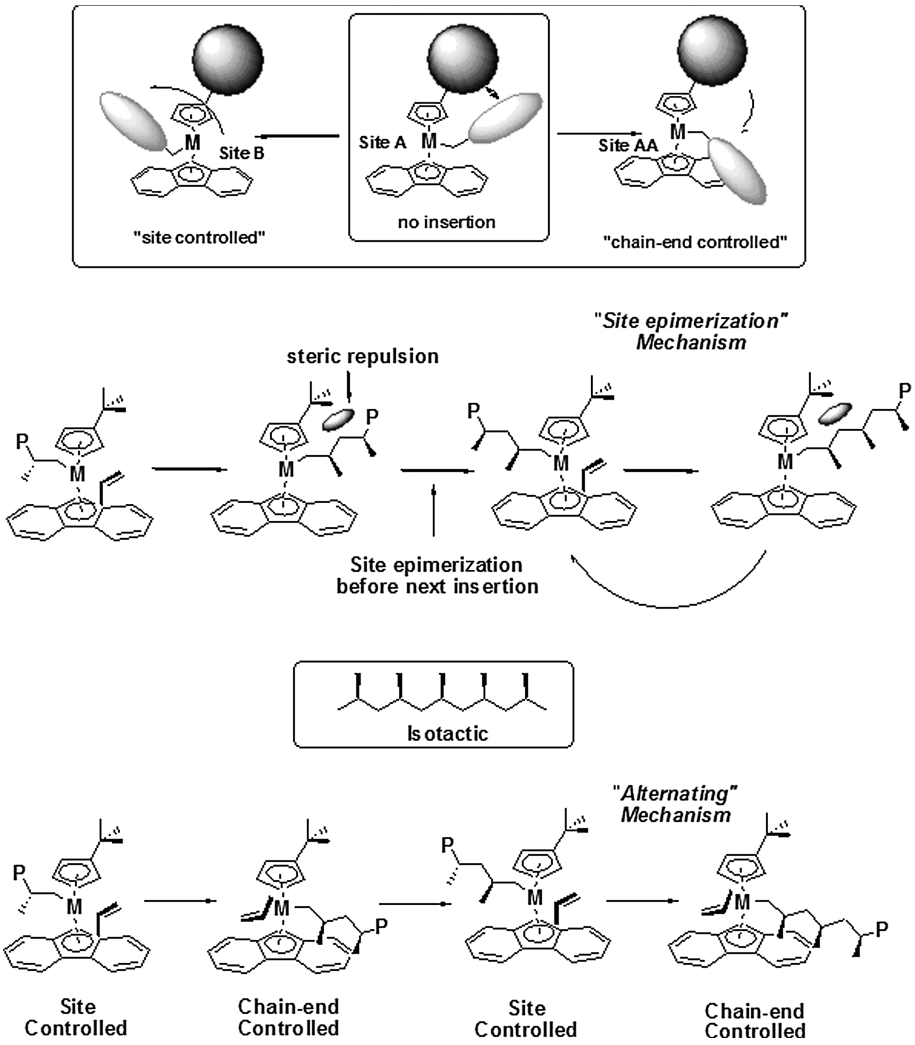

Figure 1.28 Formation of isotactic polypropylene (iPP) from a C_1 symmetric metallocene.

the growing polymer chain is located on the crowded (*tert*-butyl) side of the metallocene. Steric repulsion forbids subsequent insertion, and so forces a site epimerization to occur (Site A to B). This leads to an inversion of the stereochemistry at the metal center and a re-formation of the initial enantioselective site. Propagation then continues via this two step process (insertion–"back-skip"–insertion, etc.) to form isotactic polypropylene.

In the "alternating" mechanism, insertion occurs at the enantioselective and aselective sites of the metallocene. Insertion occurs at the enantioselective site (Site B, Figure 1.28), after which an available site becomes open due to a redirection of the growing polymer chain away from the steric bulk of the *tert*-butyl moiety and

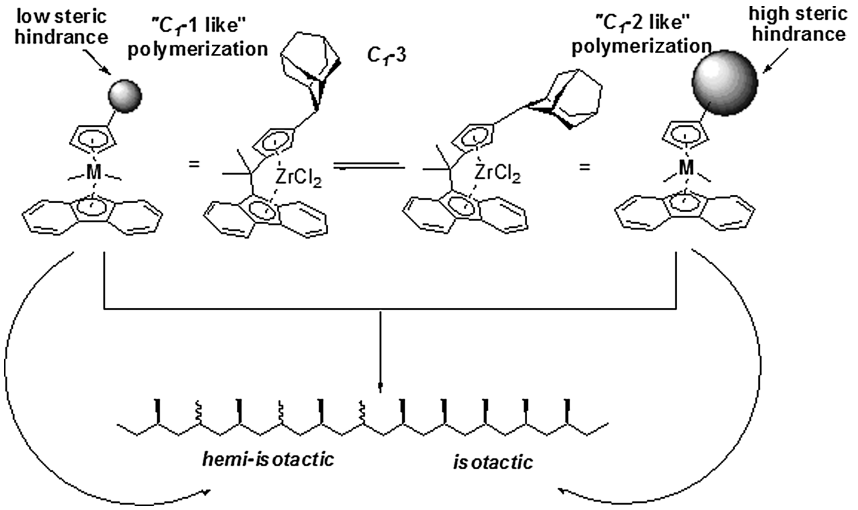

Figure 1.29 Formation of hemi-isotactic-*co*-isotactic stereoblock copolymers.

towards the fluorenyl group (Site A to AA). Insertion of the next monomer occurs with a *trans* arrangement between the polymer chain and the methyl group of the propylene monomer. Isotactic enchainment of propylene then continues via an *alternating* enantiomorphic site-controlled and chain-end-controlled mechanism [88].

The formation of hemi-isotactic-*co-isotactic* stereo-block polypropylene from C_2-2 can then be rationalized in terms of the adamantly ligand "oscillating" between positions that exert high or low steric hindrance of the growing polymer chain, within the time frame of polymer growth (Figure 1.29) [87].

The copolymerization of ethylene and propylene with bridged metallocenes $Me_2E(3\text{-}RCp)(Flu)X_2$/MAO (E = C, X = Me; E = Si, X = Cl; R = H or alkyl) have also been investigated [89]. Ethylene/propylene copolymerization with metallocenes having heterotopic active sites (R = Me, *i*-Pr) yield alternating, isotactic ethylene/propylene copolymers. Both, the nature of the substituent R and the bridging atom (E) influenced the copolymerization behavior, including copolymerization activity, copolymer sequence distribution, molecular weight, and stereochemistry.

1.3.3.2 Ethylene

Iron 2,6-bis(arylimino)pyridyl Complexes The Brookhart–Gibson family of 2,6-bis(arylimino)pyridyl iron complexes are effective catalysts for the conversion of ethylene either to highly-linear HDPE or to linear α-olefins with Schulz–Flory distribution, depending on the aryl group on the imine moiety [90]. For linear HDPE, the conditions are that the aryl rings bear either alkyl/aryl groups on both *ortho*-positions or a large alkyl group, such as *tert*-butyl, on an *ortho*-position. The presence of *ortho*-substituents locks the aryl groups orthogonal to the N–N–N plane (Figure 1.30), and also on the timescale of polymerization, which induces a

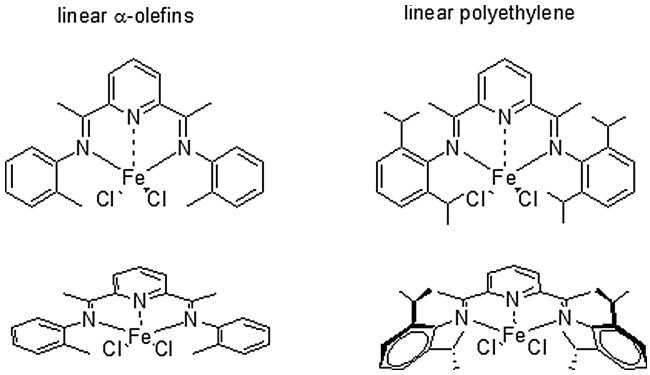

Figure 1.30 Ligand bonding patterns and its affects on the molecular weight capabilities of 2,6-bis(arylimino)pyridyl iron complexes.

retarding effect on the chain-transfer rate. Typically, the steric bulk of the aryl *ortho*-substituents affects the productivity and the polymer's molecular weight. A general rule of thumb is that an increased steric bulk increases the molecular weight by (retarded chain transfer, as discussed above), but decreases productivity. The HDPEs produced by 2,6-bis(arylimino)pyridyl Fe(II) catalysis exhibit high melting points (133–139 °C) accompanied by remarkably high heats of fusion (ΔH = 220–230 J g^{-1}); improved stiffness, high densities and gas permeability are also claimed. The absence of branches on the polymer chains indicates that the Fe(II) polymerization catalysts are unable to isomerize the produced alkyl via a "chain-walking" mechanism, nor to incorporate early-produced α-olefins into the growing polymer chain (SCB or LCB) [91].

Iron 2,6-bis(arylimino)pyridyl complexes in combination with MAO and $ZnEt_2$ (>500 equiv.) have been shown by Gibson and coworkers to catalyze polyethylene chain growth on zinc [92]. The catalyzed chain growth process is characterized by an exceptionally fast and reversible exchange of the growing polymer chains between the iron and zinc centers. Upon hydrolysis of the resultant ZnR_2 product, a Poisson distribution of linear alkanes is obtained; linear α-olefins with a Poisson distribution can be generated via a nickel-catalyzed displacement reaction. The remarkably efficient iron-catalyzed chain growth reaction for $ZnEt_2$ compared to other metal alkyls can be rationalized on the basis of: (i) relatively low steric hindrance around the zinc center; (ii) their monomeric nature in solution; (iii) the relatively weak Zn–C bond; and (iv) a reasonably close match in Zn–C and Fe–C bond strengths.

Nickel α-Diimine The physical properties of the homopolyethylenes produced by these catalyst systems vary widely depending on the type and extent of branching and polymer molecular weight. It is clear from various studies that structural variations of the α-diimine ligand coupled with the conditions of polymerization (temperature and ethylene pressure) can be used to control branching and molecu-

lar weight in a "predictable" way (Figure 1.31). Thus, variably branched polyethylenes can be produced without the use of an additional α-olefin comonomer (as is required for early metal catalysts) with properties that not only span the range of HDPE to LLDPE to LDPE but also include amorphous, elastomeric homopolymers [55, 93, 94].

In the chain-walking mechanism, the active center moves along the growing polymer chain (Figure 1.32). The process commences when a β-hydride transfer is followed by reinsertion, instead of a monomer addition. In this process the active site moves from the terminal carbon in the polymer chain to the next carbon in the backbone. This chain-walking step can be repeated several times before a monomer is added to the chain or the chain is terminated. A monomer insertion after a chain-walking step produces a branch. Figure 1.32 illustrates a simplified scheme of this mechanism. Chain walking is believed to occur in both directions – that is, from the terminal carbon towards the center of the backbone, and from any internal carbon backward to the terminal carbon. For nickel-diimine systems there is no evidence of branches on branches or branches separated by only one carbon, whilst a different behavior has been observed for palladium-α-diimine-catalyzed polyethylene, which does possess branches on branches.

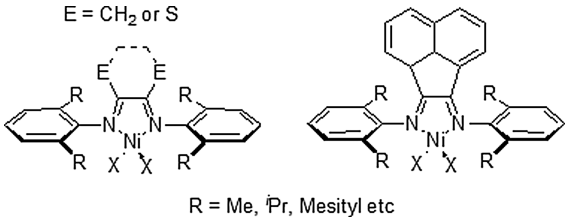

Figure 1.31 Nickel α-diimine.

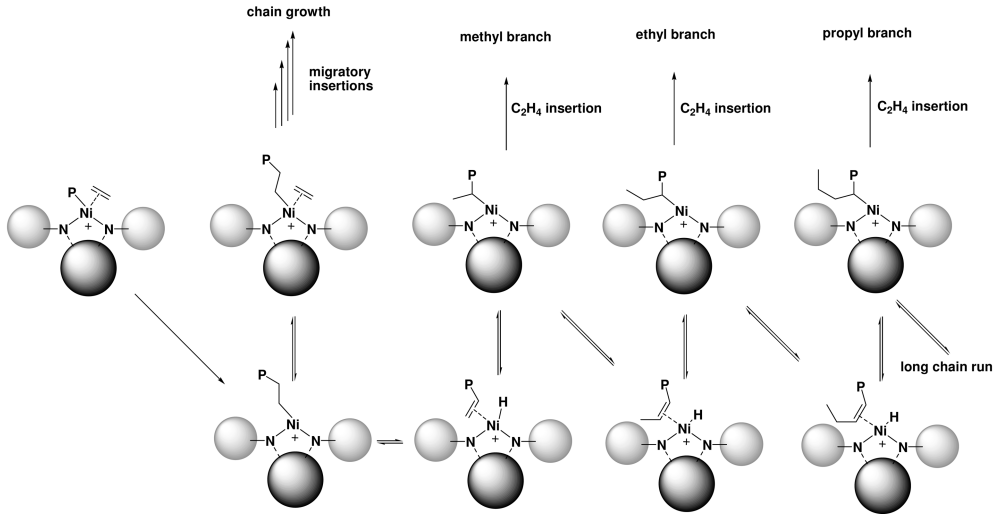

Figure 1.32 Chain-walking mechanism.

Due to the kinetics of chain transfer, several generalized trends can be used for tailoring the polymer. Increasing the steric bulk of the *ortho* aryl substituents on the α-diimine ligand increases the molecular weights of the polyethylenes. It also increases the extent of branching, as well as the turnover frequency (TOF). The electron-withdrawing substituents, such as *o*-CF_3, appear to increase the TOF more than expected, based simply on steric effects. Catalysts bearing alkyl substituents on the backbone carbon atoms tend to produce higher-molecular-weight polymers with narrower molecular weight distributions than do catalysts bearing the planar aromatic (acenaphthyl) backbone. Increases in ethylene pressure lead to dramatic reductions in the extent of branching in the polymer, presumably due to an increased rate of trapping and insertion relative to the rate of chain isomerization, which is independent of C_2H_4.

Increases in polymerization temperatures result in increased branching and decreased molecular weights.

1.3.4
Case Study 3: FI Catalysts; From Lazy to Hyperactive, and Beyond

The metallocene systems described above are exceptionally versatile in terms of ancillary ligand modification. However, such modification typically require numerous synthetic steps with varying degrees of selectivities and yields. The phenoxy-imine systems, as developed by Fujita and coworkers, illustrate the tremendous diversity that can be achieved in tuning the electronic and steric environment via a combination of two base component libraries [95].

The basic ligand system can be divided into two base reagents; salicylaldehydes (FI-A) and primary amines (FI-B) (Figure 1.33). The condensation of the two typically results in high selectivity and yields (hence its versatility in high-throughput developments). In addition, both reagents have a rich commercial inventory or a straightforward synthetic route. With this basic toolbox, Fujita and coworkers elegantly demonstrated the range of radically different activities, thermal stabilities, molecular weight capabilities and molecular weight distributions that could be achieved by varying combination of R_1, R_2 and R_3 groups on the final ligand.

An extraordinary increase in activity – by four to five orders of magnitude – was achieved via a relatively simple ligand modification (see Figure 1.34), whereby it

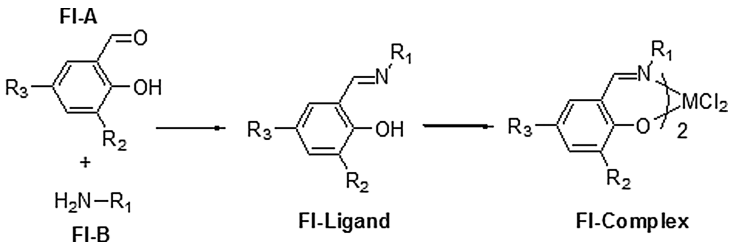

Figure 1.33 Modular synthesis of a phenoxy-imine precatalyst complex.

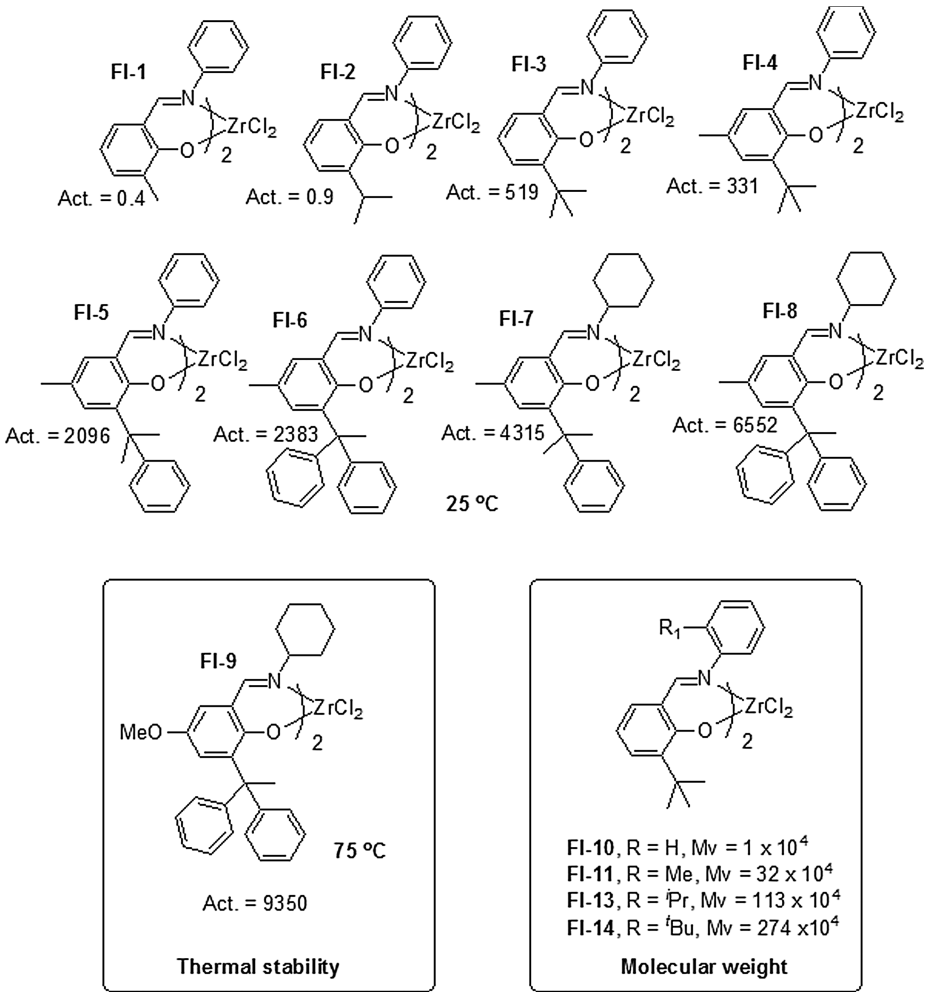

Figure 1.34 Rational design of the phenoxy-imine ligand and it affect on activity, thermal stability and molecular weight capabilities.

was demonstrated that the activity correlated directly to the steric hindrance of the R_2 substituent on the phenoxy-imine ligand (FI-ligand).

Fujita's group proposed that steric hindrance in this position protects the oxygen atom from either the coordination of Lewis acids (TMA, MAO), or the active center from typical di-nuclear deactivation processes. Improving ion-pair separation was also proposed. However, the thermal stabilities peaked at relatively low polymerization temperatures (40–50 °C) and declined rapidly at typical temperatures used in industry (above 70 °C). Poor thermal stability and activity loss was attributed to a decomposition of the active species due to a loss of the ligand(s). Once again, the group designed the ligand framework by the addition of an electron-donating

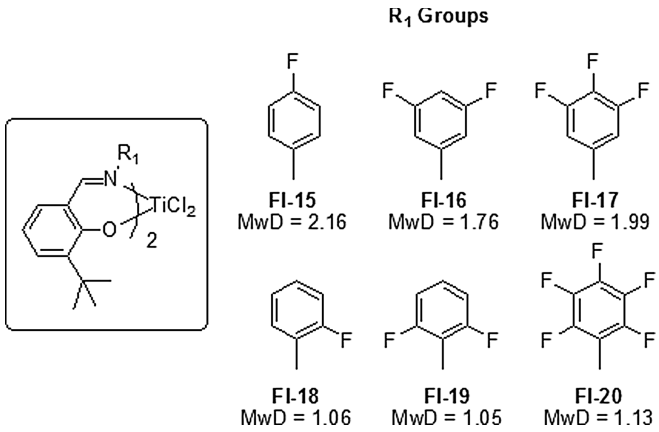

Figure 1.35 Rational design of the phenoxy-imine ligand framework to attain highly controlled ("living") polymerization of ethylene.

group in the R_3 position, thereby imparting a large electronic influence on the zirconium and strengthening the metal–ligand interactions. The synergistic benefits of fine-tuning the electronic and steric nature of the catalyst were clearly demonstrated in the performance of FI-9, which is both highly active and thermally stable.

In the process of tailoring the structure, Fujita's group also clearly demonstrated the effect of steric hindrance in the R_1 position, which increased considerably (by three orders of magnitude from FI-10 to F14) as the steric hindrance at the *ortho* position increased. The *"ortho"* effect has also been used to obtain a highly controlled polymerization. The crucial role of an *ortho*-fluorine in this process is illustrated in Figure 1.35. It has been postulated, based on computational calculations, that the *ortho*-fluorine forms an attractive interaction with the β-hydride of the growing polymer chain, making it less prone to transfer to metal and or monomer. However, recent studies by Busico have shown that the fluorine groups is not sterically benign, and that a controlled status is achieved via a "traditional" repulsive interaction, rather than via an atypical attractive interaction [96]. Whatever the reason, controlled status has been achieved and subsequently been successfully exploited by the groups of Coates and Fujita to produce mono-disperse *s*PP (via an unusual 2,1 chain-end-controlled process) and well-defined di-block copolymers of the type *s*PP-*block*-PE and *s*PP-*block*-EPR [58, 95].

1.3.5
Case Study 4: "Chain-shuttling"

Reversible transmetallation and the formation of "blocky" polyolefins are not new to the world of science [97–99]. However, until recently most tailored block structures were generated with either one type of monomer (propylene) or via a living polymerization. Although the process is extremely precise, by definition each cata-

lyst molecule produces only one polymer chain, and it is not therefore particularly economic from a "technical" polymer point of view, other than as a potential compatibilizer [58, 95].

Arriola and coworkers recently disclosed a breakthrough in polyolefin catalyst that allows the large-scale manufacture of block copolymers [57]. At the heart of the technology is a continuous solution process and a three-part catalytic system (Figure 1.36). The latter consists of a combination of two single-site catalysts (preferably post-metallocenes) which have substantially different monomer selectivities, and a reversible chain-transfer agent (CSA). For example, a zirconium

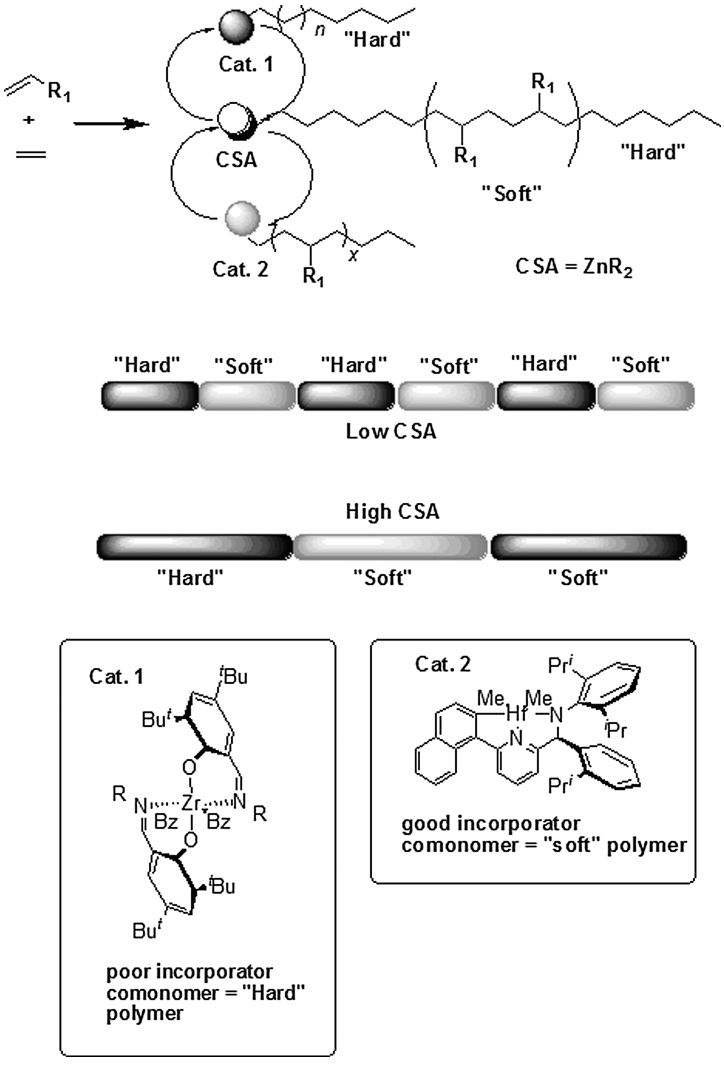

Figure 1.36 "Chain shuttling".

bis(phenoxyimine) (FI) Cat.1, which is a poor incorporator of comonomer, produces a "hard" (rigid) comonomer-lean polymer, whereas the hafnium pyridylamide (Versify™ catalyst) Cat.2 is a good incorporator of comonomer, producing a "soft" (elastomeric) comonomer-rich polymer. The diethyl zinc then intermittently "shuttles" the growing polymer chain between Cat.1 and Cat.2. The conditions and amount of chain-shuttling can be controlled so as to form block structures with longer or strong block lengths, whilst an absence of chain shuttling results in a bimodal composition. As might be imagined, a considerable amount of experimentation and tailoring was needed to optimize this reaction, and it is unsurprising that such an innovation resulted from the application of well planned high-throughput techniques.

The impressive results of catalyst tailoring are the polymeric resins that are produced with alternating blocks of the two "hard" and "soft" polymers. As mentioned above, the rate of "chain-shuttling"–and thus the "blockiness" of the product–can be controlled by the concentration of the monomers, and diethyl zinc and the resultant block-copolymer on its face offer "new-to-the-world" combinations of property performance for olefin-based elastomers. A clear example of this is the ability to "decouple" the modulus from the melting point. Compared to statistical ethylene–octene copolymers, the blocky architecture imparts a substantially higher crystallization temperature, a higher melting temperature, and a better-organized crystalline morphology, while maintaining a lower glass transition temperature. The differences between blocky and statistical copolymers become progressively more apparent as the total comonomer content increases. The high melting point versus mono-modal metallocene grade PE at the same density (120 °C versus *m*PE 60 °C at density 870 g dm^{-3}) results in an enhanced balance between flexibility and heat resistance. Additional improved properties are higher abrasion resistance, a higher recovery after elongation, a strong compression performance, and faster set-up times [100].

1.4 Immobilizing "Single-site" Olefin Polymerization Catalysts: The Basic Problems

A single-site olefin polymerization catalyst is a well-defined molecular entity which is intolerant to virtually everything, and which has a performance that is critically dependent on the precise ligand environment of the transition metal center. Therefore, immobilizing one such catalyst on a suitable solid or glassy inorganic or organic matrix is a formidably complicated task. Apart from the requirements for the support, which must be harmless to the catalyst (and also to the polymer end-user!) and amenable to morphology control (with the related delicate issues of shape replication, fragmentation and heat/mass transfer properties, etc.), the main difficulty is how to introduce a strong, non-labile binding between the support and the active species without altering (deteriorating) the performance of the latter.

Although the possible strategies (e.g., physical or chemical adsorption, tethering, etc.) will be introduced and discussed in detail in various chapters of this book, at this point it is worth mentioning a few basic problems of general relevance.

Catalyst Productivity For an efficient catalytic action, it is mandatory that the monomer has an easy access to the active sites. Selective catalysts have an active pocket which fits tightly to the incoming monomer. The crucial importance of a poorly coordinating counter-anion for cationic catalysts was mentioned previously. In view of all this, it can be understood that the introduction of a strong link between the catalyst and support, without limiting the accessibility of the active sites, is extremely complicated. In fact, the productivity of most immobilized catalysts is one or more orders of magnitude lower than that of the same catalysts in solution, though there are some exceptions. One advantage of immobilized catalysts, on the other hand, is that intermolecular catalyst deactivation processes which may be highly detrimental in solution are usually frozen on surfaces; therefore, if a good productivity can be achieved it tends to be maintained for a longer reaction time.

Catalyst Selectivity The proximity to a surface inevitably represents a perturbation to the catalyst active pocket, not only in terms of accessibility but also of symmetry. In particular, the stereoselectivity of C_s-symmetric and C_1-symmetric catalysts can be altered by the immobilization, because this may change the relative monomer insertion frequency at the two sites. One limiting case which has been reported is that of propene polymerization at certain C_s-symmetric *ansa*-zirconocene catalysts, which is syndiotactic-selective in solution but may be isotactic-selective on a surface because one side of the catalyst would be obstructed by the support. C_2-symmetric catalysts with homotopic sites are expected to be relatively insensitive to this problem; however, in case of a severe decrease of insertion rate, a loss in stereoselectivity may result due to an increased impact of growing chain epimerization (*vide infra*).

Competing Reaction Processes Immobilizing a single-site catalyst affects the kinetics of *all* reactions occurring at that catalyst, including (poly-)insertion, chain transfer, and isomerization processes. It is very unlikely that such an effect would be proportional for all such processes (some of which are intramolecular), and therefore it is to be expected that some microstructural features of the polymer produced (e.g., long and/or short branches, terminal unsaturations, average molecular mass and molecular mass distribution, regiodefects, etc.) will change upon catalyst immobilization. Of course, this also holds true for copolymerization statistics.

References

1 W. Neißl, M. Gahleitner, *Macromol. Symp.* 2002, *181*, 177.
2 V. Busico, R. Cipullo, *Prog. Polym. Sci.* 2001, *26*, 443.
3 D.M. Connor, S.D. Allen, D.M. Collard, C.L. Liotta, D.A. Schiraldi, *J. Appl. Polym. Sci.* 2001, *80*, 2696.
4 M. Gahleitner, *Prog. Polym. Sci.* 2001, *26*, 895.
5 N.J. Inkson, T.C.B. McLeish, O.G. Harlen, D.J. Groves, *J. Rheol.* 1999, *43*, 873.
6 J.A. Pople, G.R. Mitchell, S.J. Sutton, A.S. Vaughan, C.K. Chai, *Polymer* 1999, *40*, 2769.

7 G.H. Michler, *Polym. Adv. Technol.* 1998, *9*, 812.

8 M. Slouf, G. Radonjic, D. Hlavata, A. Sikora, *J. Appl. Polym. Sci.* 2006, *101*, 2236.

9 G. Eder, H. Janeschitz-Kriegl, *Structure development during processing. 5. Crystallization. Materials and Technology Series*, Verlag Chemie-Wiley, Weinheim, 1997, pp. 269–342.

10 M. Gahleitner, P. Jääskeläinen, E. Ratajski, C. Paulik, J. Reussner, J. Wolfschwenger, W. Neißl, *J. Appl. Polym. Sci.* 2005, *95*, 1073.

11 G. Eder, *Non-isothermal Polymer Crystallization*, in: A.J. Ryan (Ed.), *Polymers and Materials Chemistry, Encyclopedia of Materials: Science and Technology*, Vol. *V*, 2002, pp. 6213–6218.

12 S. Rabiej, B. Goderis, J. Janicki, V.B.F. Mathot, M.H.J. Koch, G. Groeninckx, H. Reynaers, J. Geland, A. Włochowicz, *Polymer* 2004, *45*, 8761.

13 B. Pukánszky, I. Mudra, P. Staniek, *J. Vinyl. Addit. Technol.* 1997, *3*, 53.

14 R. Phillips, G. Herbert, J. News, M. Wolkowicz, *Polym. Eng. Sci.* 1994, *34*, 1731.

15 B. Fillon, B. Lotz, A. Thierry, J.C. Wittmann, *J. Polym. Sci. B: Polym. Phys.* 1993, *31*, 1407.

16 M. Gahleitner, J. Wolfschwenger, K. Bernreitner, W. Neißl, C. Bachner, *J. Appl. Polym. Sci.* 1996, *61*, 649.

17 C. Grein, *Adv. Polym. Sci.* 2005, *188*, 43.

18 M. Seki, D.W. Thurman, J.P. Oberhauser, J.A. Kornfield, *Macromolecules* 2002, *35*, 2583.

19 R. Phillips, G. Herbert, J. News, M. Wolkowicz, *Polym. Eng. Sci.* 1994, *34*, 1731.

20 V. Brucato, S. Piccarolo, V. La Carrubba, *Chem. Eng. Sci.* 2002, *57*, 4129.

21 A. Van der Wal, R. Nijhof, R.J. Gaymans, *Polymer* 1998, *39*, 6781.

22 B. Pukanszky, F.H.J. Maurer, *Polymer* 1995, *36*, 1617.

23 Z. Bartczak, A.S. Argon, R.E. Cohen, M. Weinberg, *Polymer* 1999, *40*, 2331, 2347, 2367.

24 C. Grein, K. Bernreitner, A. Hauer, M. Gahleitner, W. Neißl, *J. Appl. Polym. Sci.* 2003, *87*, 1702.

25 L.A. Utracki, M.R. Kamal, *Polym. Eng. Sci.* 1982, *22*, 96.

26 M. Rätzsch, M. Arnold, E. Borsig, H. Bucka, N. Reichelt, *Prog. Polym. Sci.* 2002, *27*, 1195.

27 J. Kolařík, J. Jančář, *Polymer* 1992, *33*, 4961.

28 S.S. Ray, M. Okamato, *Prog. Polym. Sci.* 2003, *28*, 1539.

29 G. Kalay, R.A. Sousa, R.L. Reis, A.M. Cunha, M.J. Bevis, *J. Appl. Polym. Sci.* 1999, *73*, 2473.

30 I.M. Ward, P.J. Hine, *Polymer* 2004, *45*, 1423.

31 L. Resconi, J.C. Chadwick, L. Cavallo, in: D.M.P. Mingos, R. Crabtree, R. (Eds.), *Comprehensive, Organometallic Chemistry III*, Elsevier, New York, 2007.

32 J. Scheirs, W. Kaminsky (Eds.), *Metallocene-Based Polyolefins, Preparation, Properties and Techniques*, Wiley, New York, 1999.

33 G.M. Benedikt, B.L. Goodall (Eds.), *Metallocene Catalyzed Polymers*, William Andrew Publishing, New York, 1998.

34 G.M. Benedikt (Ed.), *Metallocene Technology and Modern Methods in Commercial Applications Catalyzed Polymers*, William Andrew Publishing, New York, 1998.

35 B. Reiger, L. Saunders-Bauch, S. Kacker, S. Striegler (Eds.), *Late Transition Metal Polymerization Catalysts*, Wiley-VCH, Weinheim, 2003.

36 K. Soga, M. Terano (Eds.), *Catalyst Design for Taylor-made Polyolefins, Studies in Surface Science and Catalysis*, Elsevier, Amsterdam, 1994, Vol. *89*, p. 277.

37 A.O. Patil, G. Hlatky (Eds.), *Beyond Metallocenes: Next-Generation Polymerization Catalysts*, ACS Symposium Series 857, Oxford University Press, 2004.

38 G.G. Hlatky, *Coord. Chem. Rev.* 1999, *181*, 243.

39 P.J. Shapiro, *Coord. Chem. Rev.* 2002, *231*, 67.

40 M. Bochmann, *J. Organomet. Chem.* 2004, *689*, 3982.

41 J.-N. Pédeutour, K. Radhakrisknan, H. Cramail, A. Deffieux, *Macromol. Rapid Commun.* 2001, *22*, 1095.

42 E.Y.-X. Chen, T. Marks, *Chem. Rev.* 2000, *100*, 1391.

43 E. Zurek, T. Ziegler, *Prog. Polym. Sci.* 2004, *29*, 107.

44 F. Focante, P. Mercandelli, A. Sironi, L. Resconi, *Coord. Chem. Rev.* 2006, *250*, 170.

45 S. Tomasi, A. Razavi, T. Ziegler, *Organometallics* 2007, *26*, 2024.

46 M.-C. Chen, J.A.S. Roberts, T.J. Marks, *J. Am. Chem. Soc.* 2004, *126*, 4605.

47 P.A. Wilson, M.H. Hannant, J.A. Wright, R.D. Cannon, M. Bochmann, *Macromol. Symp.* 2006, *236*, 100.

48 V. Busico, V. van Axel Castelli, P. Aprea, R. Cipullo, A. Segre, G. Malarico, M. Vacatello, *J. Am. Chem. Soc.* 2003, *125*, 5451.

49 G. Fink, R. Rottler, R. Mynott, W. Fenzel, *Angew. Makromol. Chem.* 1987, *154*, 1.

50 Z. Liu, E. Somsook, C.B. White, K.A. Rosaaen, C.R. Landis, *J. Am. Chem. Soc.* 2001, *123*, 11193.

51 E.J. Arlman, P. Cosse, *J. Catal.* 1964, *3*, 99.

52 (a) M. Brookhart, M.L.H. Green, *J. Organomet. Chem.* 1983, *250*, 395; (b) D. T. Laverty, J.J. Rooney, *J. Chem. Soc., Faraday Trans. I* 1983, *79*, 869.

53 L. Izzo, L. Caporaso, G. Senatore, L. Olivia, *Macromolecules* 1999, *33*, 6913.

54 R. Schubbe, K. Angermund, G. Fink, R. Gooddard, *Macromol. Chem. Phys.* 1995, *196*, 478.

55 S.D. Ittel, L.K. Johnson, M. Brookhart, *Chem. Rev.* 2000, *100*, 1169.

56 A.L. McKnight, R.M. Waymouth, *Chem. Rev.* 1998, *98*, 2587.

57 D.J. Arriola, E.M. Carnahan, P.D. Hustad, R.L. Kuhlman, T.T. Wenzel, *Science* 2006, *312*, 714.

58 (a) G.J. Domski, J.M. Rose, G.W. Coates, A.D. Bolig, M. Brookhart, *Prog. Polym. Sci.* 2007, *32*, 30; (b) G.W. Coates, P.D. Hustad, S. Reinartz, *Angew. Chem. Int. Ed.* 2002, *41*, 2236.

59 V. Busico, R. Cipullo, *Prog. Poly. Sci.* 2001, *26*, 443.

60 L. Resconi, L. Cavallo, A. Fait, F. Piemontesi, *Chem. Rev.* 2000, *100*, 1253.

61 G.W. Coates, *Chem. Rev.* 2000, *100*, 1223.

62 K. Angermund, G. Fink, V.R. Jensen, R. Kleinschmidt, *Chem. Rev.* 2000, *100*, 1457.

63 (a) C.L. Landis, D.R. Sillars, J. Batterton, *J. Am. Chem. Soc.* 2004, *126*, 8890; (b) V. Busico, R. Cipullo, V. Romanelli, S. Ronca, M. Togrou, *J. Am. Chem. Soc.* 2005 *127*, 1608. Further reading on "dormant site" generation follow secondary insertion.

64 (a) T. Shiono, S.M. Azad, T. Ikeda, *Macromolecules* 1999, *32*, 5723; (b) W. Weng, E.J. Markel, A.H. Dekmezian, *Macromol. Chem. Phys.* 2001, *22*, 1488.

65 (a) Y. Suzuki, T. Yasumoto, K. Mashima, J. Okuda, *J. Am. Chem. Soc.* 2006, *128*, 13017; (b) P. Yang, M.C. Baird, *Organometallics* 2005, *24*, 6013; (c) P.J. Chirik, N.F. Dalleska, L.M. Henling, J.E. Bercaw, *Organometallics* 2005, *24*, 2789. Interesting additional reading on β-Me transfer.

66 For examples, see: (a) K.K. Kang, T. Shiono, T. Ikeda, *Macromolecules* 1997, *30*, 1231; (b) A.-L. Mogstad, R.M. Waymouth, *Macromolecules* 1994, *27*, 2313.

67 (a) B.A. Krenstel, Y.V. Kissin, V.J. Kleiner, L.L. Stotskaya, *Polymer and co-polymers of higher α-olefins*, Hanser Publishers, Munich, 1997; (b) J.A. Ewen, in: J. Scheirs, W. Kaminsky (Eds.), *Metallocene-Based Polyolefins, Preparation, Properties and Techniques*, Wiley, New York, 1999.

68 J. Shum, M.J. Schneider, R. Mülhaupt, *J. Mol. Catal.* 1998, *128*, 215.

69 J.A. Ewen, *J. Am. Chem. Soc.* 1984, *106*, 6355.

70 G. Natta, I. Pasquon, A. Zimbelli, *J. Am. Chem. Soc.* 1962, *82*, 1488.

71 J.A. Ewen, *J. Mol. Catal. A: Chemistry* 1998, *128*, 103.

72 (a) D. Fischer, R. Mulhaupt, *Makromol. Chem. Phys.* 1994, *195*, 1143; (b) P. Viville, D. Daoust, A.M. Jonas, B. Nysten, R. Legras, M. Dupire, J. Michel, G. Debras, *Polymer* 2001, *42*, 1953.

73 J.A. Ewen, R.L. Jones, A. Razavi, J.D. Ferrara, *J. Am. Chem. Soc.* 1998, *110*, 6255.

74 F.R.W.P. Wild, L. Zsolani, G. Huttner, H.-H. Brintzinger, *J. Organomet. Chem.* 1982, *232*, 233.

75 J.A. Ewen, *J. Am. Chem. Soc.* 1984, *106*, 6355.

76 W. Kaminsky, K. Külper, H.-H. Brintzinger, *Angew. Chem., Int. Ed.* 1985, *24*, 507.

77 W. Spaleck, F. Küber, A. Winter, J. Rohrmann, B. Bachmann, M. Antberg, V. Dolle, E. Paulus, *Organometallics* 1994, *13*, 954.

78 N. Kashiwa, S. Nojoh, J. Imuta, T. Tsutsui, in: W. Kaminsky (Ed.), *Metalorganic Catalysts for Synthesis and Polymerization*, Springer-Verlag, Berlin, 1999, p. 30.

79 A. Winter, Maack Polypropylene Conference, Zurich, 2006. Congress papers available online from Maack Business Services (http://www.mbspolymer.com/).

80 J.A. Ewen, A. Zambelli, P. Longo, J.M. Sullivan, *Macromol. Rapid Commun.* 1998, *19*, 71.

81 J.A. Ewen, M.J. Elder, R.L. Jones, A.L. Rheingold, L.M Liable-Sands, R.D. Sommer, *J. Am. Chem. Soc.* 2001, *123*, 4763.

82 C. De Rosa, F. Auriemma, A. Di Capua, L. Resconi, S. Guidotti, I. Camurati, I.E. Nifant'ev, P. Laishevtsev, *J. Am. Chem. Soc.* 2004, *126*, 17040.

83 P. Walter, J. Heinemann, H. Ebeling, D. Mäder, S. Trinkle, R. Mülhaupt, in: R. Blom, A. Follestad, E. Rytter, M. Tilset, M. Ystenes (Eds.), *Organometallic Catalysts and Olefin Polymerisation*, Springer-Verlag, Berlin, 2001, p. 319.

84 J.A. Ewen, M.J. Elder, R.L. Jones, L. Haspeslagh, J.L. Atwood, S.G. Bott, K. Robinson, *Makromol. Chem. Makromol Symp.* 1991, *48–49*, 235.

85 (a) S. Miyake, Y. Okumura, S. Inazawa, *Macromolecules* 1995, *28*, 3074; (b) A. Razavi, D. Vereecke, L. Peters, K. Den Dauw, L. Nafpliotis, J.L. Atwood, in: G. Fink, R. Mülhaupt, H.-H. Brintzinger (Eds.,) Ziegler Catalysts, Springer-Verlag, Berlin, 1995, p. 111; (c) A. Razavi, U. Thewalt, *Coord. Chem. Rev.* 2006, *250*, 155.

86 S.A. Miller, J.E. Bercaw, *Organometallics* 2002, *21*, 934.

87 A. Razavi, J.L. Atwood, *J. Organomet. Chem.* 1993, *459*, 117.

88 S.A. Miller, J.E. Bercaw, *Organometallics* 2006, *25*, 3576.

89 W. Fan, M.K. Leclerc, R.M. Waymouth, *J. Am. Chem. Soc.* 2001, *123*, 9555.

90 V.C. Gibson, S.K. Spitzmesser, *Chem. Rev.* 2003, *103*, 283.

91 C. Bianchini, G. Giambastiani, I.G. Rios, G. Mantovani, A. Meli, A.M. Segarra, *Coord. Chem. Rev.* 2006, *250*, 1391.

92 G.J.P. Britovsek, S.A. Cohen, V.C. Gibson, M. van Meurs, *J. Am. Chem. Soc.* 2004, *126*, 10701.

93 D.P. Gates, S.A. Svejda, E. Oñate, C.M. Killian, L.K. Johnson, P.S. White, M. Brookhart, *Macromolecules* 2000, *33*, 2320.

94 D. Meinhard, M. Wegner, G. Kipiani, A. Hearley, P. Reuter, S. Fischer, O. Marti, B. Rieger, *J. Am. Chem. Soc.* 2007, *129*, 918.

95 H. Makio, N. Kashiwa, T. Fujita, *Adv. Synth. Catal.* 2002, *344*, 477.

96 V. Busico, G. Talarico, R. Cipullo, *Macromol. Symp.* 2005, *226*, 1.

97 J.C.W. Chien, Y. Iwamoto, M.D. Rausch, W. Wedler, H.H. Winter, *Macromolecules* 1997, *30*, 3447.

98 S. Lieber, H.-H. Brintzinger, *Macromolecules* 2000, *33*, 9192.

99 C. Pryzbyla, G. Fink, *Acta Polym.* 1999, *50*, 77.

100 H.P. Wang, D.U. Khariwala, W. Cheung, S.P. Chum, A. Hiltner, E. Baer, *Macromolecules* 2007, *40*, 2852.